Docket No.: HO-P02070US1

Utility Application

I hereby certify that this correspondence is being deposited with the U.S. Postal Service as Express Mail, Airbill No. EU186312116US, in an envelope addressed to: Box Patent Application, Commissioner for Patents, Washington, DC 20231, on the date shown below.

Dated: 01/15/02

Signature:

### IN THE UNITED STATES PATENT AND TRADEMARK OFFICE

### APPLICATION FOR U.S. LETTERS PATENT

Title:

THERMODYNAMIC PROPENSITIES OF AMINO ACIDS IN THE NATIVE STATE ENSEMBLE: IMPLICATIONS FOR FOLD RECOGNITION

Inventors:

Vince Hilser and Robert O. Fox

Thomas D. Paul FULBRIGHT & JAWORSKI L.L.P. 1301 McKinney, Suite 5100 Houston, Texas 77010-3095 (713) 651-5407

## THERMODYNAMIC PROPENSITIES OF AMINO ACIDS IN THE NATIVE STATE ENSEMBLE: IMPLICATIONS FOR FOLD RECOGNITION

[0001] This Applications claims priority to U.S. Provisional Application No. 60/261,733, which was filed on January 16, 2001.

[0002] The work herein was supported by grants from the United States Government. The United States Government may have certain rights in the invention.

### **BACKGROUND OF THE INVENTION**

#### I. Field of the Invention

[0003] The present invention relates to the field of structural biology. More particularly, the present invention relates to a protein database and methods of developing a protein database that contains all of the thermodynamic information necessary to encode a three-dimensional protein structure.

#### II. Related Art

[0004] It is a longstanding idea that protein structures are the result of an amino acid chain finding its global free energy minimum in the solvent environment (Anfinsen, 1973). Several exceptions to this so-called "thermodynamic control" have been discovered in recent years, including examples of proteins whose folding may be under "kinetic control" (Baker et al., 1992, Cohen, 1999) and proteins requiring information not completely contained in the amino acid sequence (e.g., chaperone-assisted folding (Feldman & Frydman 2000, Fink 1999)). Although thermodynamic control is widely accepted as the default behavior for correct folding (Jackson, 1998), a detailed understanding of the forces involved in thermodynamic control and how atomic interactions relate amino acid sequence to the folding and stability of the native structure has still proven elusive.

[0005] Despite the progress that has been made in protein folding, obstacles have prevented an accurate structure prediction algorithm. An obstacle in developing an accurate structure prediction algorithm has been the lack of suitable potentials for calculating the free energies of different conformations of a given protein molecule. In 1992, high-pressure liquid chromatography (HPLC) was used to quantitate the energies of pairwise interactions between amino acid side chains (Pochapsky and Gopen, 1992). Yet further, in 1999, Pochapsky used HPLC to further study the thermodynamic interactions between amino acid side chains. A stationary phase was prepared for use in an HPLC. The phase was 25112195.1

prepared by derivatizing microparticulate silica gels with functionality mimicking the side chain of hydrophobic and amphiphilic amino acid analytes (Pereira de Araujo *et al.*, 1999). Thus, this variation of an HPLC method compares entropies and free energies of interaction using different derivatized microparticulate silica gels.

[0006] The present invention uses a computer-based algorithm to address for the first time whether amino acid residue types have distinct preferences for thermodynamic environments in the folded native structure of a protein, and whether a scoring matrix based solely on thermodynamic information (independent of explicit structural constraints) can be used to identify correct sequences that correspond to a particular target fold. This is done by means of a unique approach in which the regional stability differences within a protein are determined for a database of proteins using the COREX algorithm (Hilser & Freire, 1996). The COREX algorithm generates an ensemble of states using the high-resolution structure as a template. Based on the relative probability of the different states in the ensemble, different regions of the protein are found to be more stable than others. Thus, the COREX algorithm provides access to residue-specific free energies of folding.

### BRIEF SUMMARY OF THE INVENTION

[0007] One embodiment of the present invention is directed to a system and method of developing a protein database that contains all of the thermodynamic information necessary to encode a three-dimensional protein structure

[0008] Another embodiment of the present invention comprises a protein database comprising nonhomologus proteins having known residue-specific free energies of folding of the proteins. In specific embodiments, the database comprises globular proteins.

[0009] In further embodiments, the database is determined by a computational method comprising the step of determining a stability constant from the ratio of the summed probability of all states in the ensemble in which a residue j is in a folded conformation to the summed probability of all states in which j is in an unfolded conformation according to the equation,

$$K_{f,j} = \frac{\sum P_{f,j}}{\sum P_{nf,j}}$$

[0010] Another specific embodiment of the present invention comprises that the stability constants for the residues are arranged into at least one of the three thermodynamic classification groups selected from the group consisting of stability, enthalpy, and entropy.

- [0011] In specific embodiments, the stability thermodynamic classification group comprises high stability, medium stability and low stability. More particularly, the residues in the high stability classification comprises phenylalanine, tryptophan and tyrosine. The residues in the low stability classification comprises glycine and proline. And the residues in the medium stability classification comprises asparagine and glutamic acid.
- [0012] Yet further, the enthalpy thermodynamic classification group comprises high enthalpy and low enthalpy. Enthalpy comprises a ratio of the contributions of polar and apolar components.
- [0013] In another specific embodiment, the entropy thermodynamic classification group comprises high entropy and low entropy. Entropy comprises a ratio of the contributions of polar and apolar components.
- [0014] In a further embodiment, the stability constants for the residues are arranged into twelve thermodynamic classifications selected from the group consisting of HHH, MHH, LHH, MHL, LHL, HLL, MLL, HLH, MLH and LLH.
- [0015] Another embodiment of the present invention is a method of developing a protein database comprising the steps of: inputting high resolution structures of proteins; generating an ensemble of incrementally different conformational states by combinatorial unfolding of a set of predefined folding units in all possible combinations of each protein; determining the probability of each said conformational state; calculating a residue-specific free energy of each said conformational state; and classifying a stability constant into at least one thermodynamic classification group selected from the group consisting of stability, enthalpy, and entropy. Specifically, the protein database comprises globular and nonhomologous proteins.

[0016] In specific embodiments, the generating step comprises dividing the proteins into folding units by placing a block of windows over the entire sequence of the protein and sliding the block of windows one residue at a time.

[0017] In further specific embodiment, the determining step comprises determining the free energy of each of the conformational states in the ensemble; determining the Boltzmann weight  $[K_i = \exp(-\Delta G_i/RT)]$  of each state; and determining the probability of each state using the equation:

$$P_i = \frac{K_i}{\sum K_i'}$$

[0018] In specific embodiments, the calculating step comprises determining the energy difference between all microscopic states in which a particular residue is folded and all such states in which it is unfolded using the equation

$$\Delta G_{f,j} = -RT \cdot ln\kappa_{f,j}$$

[0019] Another embodiment of the present invention is a method of identifying a protein fold comprising determining the distribution of amino acid residues in different thermodynamic environments corresponding to a known protein structure. Specifically, determining the distribution of amino acid residues comprises constructing scoring matrices derived of thermodynamic information. The scoring matrices are derived from COREX thermodynamic information selected from the group consisting of stability, enthalpy, and entropy.

[0020] The aforementioned embodiments of the present invention may be readily implemented as a computer-based system. One embodiment of such a computer-based system includes a computer program that receives an input of high resolution structure data for one or more proteins. The computer-based program utilizes this data to determine the amino acid thermodynamic classifications for the proteins. These amino acid thermodynamic classifications may then be stored in a database. The database of the system preferably has a data structure with a field or fields for storing a value for an amino acid name or amino acid abbreviation, and one or more classification fields for storing a numerical value for a thermodynamic classification for a particular amino acid. Additionally, this data

structure may have a field for storing a value representing the summed total of each of the numerical values for each thermodynamic classification for a particular amino acid.

program performs a process to generate thermodynamic classifications for a protein which includes inputting high resolution structures of proteins, generating an ensemble of incrementally different conformational states by combinatorial unfolding of a set of predefined folding units in all possible combinations of each protein, determining the probability of each said conformational state, calculating a residue-specific free energy of each said conformational state, and classifying a stability constant into a thermodynamic classification group. Additionally, the computer-based program may have a probability determination module to determine the free energy of each of the conformational states in a computed ensemble, determine a Boltzmann weight, and then determine the probability of each state.

[0022] Moreover, the computer-based program of the inventive system may have a display/reporting module for producing one or more graphical reports to a screen or a print-out. Some of these reports include: a display of a three-dimensional protein structure based on said amino acid thermodynamic classifications; a scatter-plot of normalized frequencies of COREX stability data versus normalized frequencies of average side chain surface exposure; and a chart displaying thermodynamic environments for amino acids of a protein.

[0023] Another aspect of the inventive methods is that they may be stored as computer executable instructions on computer-readable medium.

[0024] The foregoing has outlined rather broadly the features and technical advantages of the present invention in order that the detailed description of the invention that follows may be better understood. Additional features and advantages of the invention will be described hereinafter which form the subject of the claims of the invention. It should be appreciated by those skilled in the art that the conception and specific embodiment disclosed may be readily utilized as a basis for modifying or designing other structures for carrying out the same purposes of the present invention. It should also be realized by those skilled in the art that such equivalent constructions do not depart from the spirit and scope of the invention as set forth in the appended claims. The novel features which are believed to be

5

characteristic of the invention, both as to its organization and method of operation, together with further objects and advantages will be better understood from the following description when considered in connection with the accompanying figures. It is to be expressly understood, however, that each of the figures is provided for the purpose of illustration and description only and is not intended as a definition of the limits of the present invention.

### **BRIEF DESCRIPTION OF THE DRAWINGS**

[0025] The following drawings form part of the present specification and are included to further demonstrate certain aspects of the present invention. The invention may be better understood by reference to one or more of these drawings in combination with the detailed description of specific embodiments presented herein.

[0026] Figure 1A and Figure 1B are a schematic description of the COREX algorithm applied to the crystal structure of the ovomucoid third domain, OM3 (20vo). Figure 1A summarizes the partitioning strategy of the COREX algorithm. Figure 1 B illustrates the solvent exposed surface area (ASA) contributing to the energetics of microstate 32.

predicted from COREX data with experimental values for ovomucoid third domain (20vo). Unfilled vertical bars denote predicted values, and filled vertical bars denote experimental values (Swint-Kruse & Robertson, 1996). The solid line denotes lnxf values. The simulated temperature of the COREX calculation was set at 30 °C to match the experimental conditions. Secondary structure is given by labeled horizontal lines. Asterisks show the positions of Thr 47 and Thr 49, referred to in the text.

[0028] Figure 3A, Figure 3B, Figure 3C, Figure 3D, Figure 3E, Figure 3F, Figure 3G, Figure 3H, Figure 3I, Figure 3J, Figure 3K, Figure 3L, Figure 3M, Figure 3N, Figure 3N, Figure 3O, Figure 3P, Figure 3Q, Figure 3R, Figure 3S and Figure 3T comprise normalized frequencies of COREX stability data as a function of amino acid type. Figure 3A shows the data as a function of the amino acid arginine. Figure 3C shows the data as a function of the amino acid asparagine. Figure 3D shows the data as a function of the amino acid aspartic acid. Figure 3E shows the data as a function of the amino acid cysteine. Figure 3F shows the data as a function of the amino acid glutamine. Figure 3G shows the data as a function of the amino

acid glutamic acid. Figure 3H shows the data as a function of the amino acid glycine. Figure 3I shows the data as a function of the amino acid histidine. Figure 3J shows the data as a function of the amino acid isoleucine. Figure 3K shows the data as a function of the amino acid leucine. Figure 3L shows the data as a function of the amino acid lysine. Figure 3M shows the data as a function of the amino acid methionine. Figure 3N shows the data as a function of the amino acid phenylalanine. Figure 3O shows the data as a function of the amino acid proline. Figure 3P shows the data as a function of the amino acid serine. Figure 3Q shows the data as a function of the amino acid tryptophan. Figure 3S shows the data as a function of the amino acid tryptophan. Figure 3S shows the data as a function of the amino acid tryptophan. Figure 3S shows the data as a function of the amino acid tryptophan. Figure 3D shows the data as a function of the amino acid tryptophan. Figure 3D shows the data as a function of the amino acid tryptophan. Figure 3D shows the data as a function of the amino acid tryptophan. Figure 3D shows the data as a function of the amino acid tryptophan. Figure 3D shows the data as a function of the amino acid tryptophan. Figure 3D shows the data as a function of the amino acid tryptophan. Figure 3D shows the data as a function of the amino acid tryptophan. Figure 3D shows the data as a function of the amino acid tryptophan. Figure 3D shows the data as a function of the amino acid tryptophan. Figure 3D shows the data as a function of the amino acid tryptophan. Figure 3D shows the data as a function of the amino acid tryptophan. Figure 3D shows the data as a function of the amino acid tryptophan. Figure 3D shows the data as a function of the amino acid tryptophan. Figure 3D shows the data as a function of the amino acid tryptophan. Figure 3D shows the data as a function of the amino acid tryptophan.

[0029] Figure 4 is a scatterplot of normalized frequencies of COREX stability data versus normalized frequencies of average side chain surface area exposure. Average side chain exposure in the native structure was calculated by using a moving window of five residues, similar to the basis of the COREX algorithm. These values were then binned into high, medium, and low surface area exposure.

[0030] Figure 5A, Figure 5B, Figure 5C and Figure 5D illustrate a summary of fold-recognition results for COREX stability and DSSP secondary structure scoring matrices for 44 targets. Black bars denote real data (either lnkf or secondary structure), and striped bars denote the average of three random data sets. Figure 5A shows the lnkf scoring matrix local alignment algorithm. Figure 5B shows the lnkf scoring matrix global alignment algorithm. Figure 5C shows the secondary structure scoring matrix local alignment algorithm. Figure 5D shows the secondary structure scoring matrix global alignment algorithm.

[0031] Figure 6A, Figure 6B and Figure 6C illustrate examples of successful local alignment for three targets. Results for target 1igd (Protein G) are shown in Figure 6A, results for target 1vcc (DNA topoisomerase I) are shown in Figure 6B, and results for target 2ait (tendamistat) are shown in Figure 6C. The thin black line represents COREX calculated stability data (lnkf) for the protein target. The filled circles connected by a thick black line correspond to the cumulative matrix score contributed by each residue. Scores that did not

contribute to the final score due to the rules of the local alignment algorithm (Smith & Waterman, 1981) are shown as unfilled circles connected by a thick dashed line.

[0032] Figure 7 is a correlation between stability data derived from the database of 44 proteins used in this work and stability data derived from an independent database of 50 proteins. Data on the x-axis are taken from the normalized histograms in Figure 3A-Figure 3T. Data on the y-axis are derived from an identical COREX analysis of an independent database of 3304 residues from 50 PDB structures not contained in the original database. Open circles denote the values for His, a residue type with low statistics in both databases. The dashed line represents a perfect correlation.

[0033] Figure 8A and Figure 8B illustrate the results of a COREX calculation for the bacterial cold-shock protein cspA (PDB 1mjc). Figure 8A shows a plot of calculated thermodynamic stability,  $ln\kappa_{f,j}$ , as a function of residue number for cspA. The simulated temperature was 25.0°C. Regions of relatively high, medium, and low stability, are shown in dark gray, light gray, and black, respectively. Secondary structure elements, as defined by the program DSSP, (Kabsch and Sander, 1983) are labeled. Figure 8B locates the relative calculated stabilities of each residue in the 1mjc crystal structure. Note that a given secondary structural element is predicted to have varying regions of stability, and that the most stable regions of the molecule are often, but not necessarily, within the hydrophobic core.

[0034] Figure 9A, Figure 9B and Figure 9C illustrate a description of protein structure in terms of thermodynamic environments. Figure 9A shows the thermodynamic environment classification scheme used herein. Three quantities derived from the output of the COREX algorithm, stability ( $\kappa_{f,i}$ ), enthalpy ratio ( $H_{ratio,i}$ ), and entropy ratio ( $S_{ratio,i}$ ) describe the thermodynamic environment of each residue. Figure 9B shows the 12 thermodynamic environments defined by this classification scheme in a schematic describing protein energetic phase space. Each cube represents a region dominated by certain stability, enthalpy, and entropy characteristics. Every residue position in the protein structures used herein lies somewhere within this phase space. Figure 9C shows examples of the distribution of thermodynamic environments of (Figure 9B) in three proteins with varying types and amounts of secondary structure. Note that single secondary structure elements do not exhibit unique thermodynamic environments.

8

25112195.1

[0035] Figure 10A, Figure 10B, Figure 10C, Figure 10D, Figure 10E, Figure 10F, Figure 10G, Figure 10H, Figure 10I, Figure 10J, Figure 10K and Figure 10L show 3D-1D scores relating amino acid types to 12 protein structural thermodynamic environments. The three-letter abbreviation in each panel represents the stability, enthalpic, and entropic descriptor of the thermodynamic environment. Stability is classified into high, medium and low. Entropy and enthalpy are classified into high and low. Figure 10A represents LHH, which is a protein thermodynamic environment of low stability, high polar/apolar enthalpy ratio, and high conformational entropy/Gibbs' solvation energy ratio. Figure 10B represents LHL, which is a protein thermodynamic environment of low stability, high polar/apolar enthalpy ratio, and low conformational entropy/Gibbs' solvation energy ratio. Figure 10C represents LLH, which is a protein thermodynamic environment of low stability, low polar/apolar enthalpy ratio, and high conformational entropy/Gibbs' solvation energy ratio. Figure 10D represents LLL, which is a protein thermodynamic environment of low stability, low polar/apolar enthalpy ratio, and low conformational entropy/Gibbs' solvation energy ratio. Figure 10E represents MHH, which is a protein thermodynamic environment of medium stability, high polar/apolar enthalpy ratio, and high conformational entropy/Gibbs' solvation energy ratio. Figure 10F represents MHL, which is a protein thermodynamic environment of medium stability, high polar/apolar enthalpy ratio, and low conformational entropy/Gibbs' solvation energy ratio. Figure 10G represents MLH, which is a protein thermodynamic environment of medium stability, low polar/apolar enthalpy ratio, and high conformational entropy/Gibbs' solvation energy ratio. Figure 10H represents MLL, which is a protein thermodynamic environment of medium stability, low polar/apolar enthalpy ratio, and low conformational entropy/Gibbs' solvation energy ratio. Figure 10I represents HHH, which is a protein thermodynamic environment of high stability, high polar/apolar enthalpy ratio, and high conformational entropy/Gibbs' solvation energy ratio. Figure 10J represents HHL, which is a protein thermodynamic environment of high stability, high polar/apolar enthalpy ratio, and low conformational entropy/Gibbs' solvation energy ratio. Figure 10K represents HLH, which is a protein thermodynamic environment of high stability, low polar/apolar enthalpy ratio, and high conformational entropy/Gibbs' solvation energy ratio. Figure 10L represents HLL, which is a protein thermodynamic environment of high stability, low polar/apolar enthalpy ratio, and low conformational entropy/Gibbs' solvation energy ratio.

25112195.1 9

[0036] Figure 11 shows fold-recognition results for 81 protein targets using a scoring matrix composed of thermodynamic information from protein structures. The horizontal axis represents the percentile ranking of the score against the target structure for the sequence corresponding to the target structure. For example, the sequence corresponding to the target cold-shock protein (PDB 1mjc) received the 157<sup>th</sup> highest score of 3858 sequences against the cold-shock protein thermodynamic profile. This result placed the sequence for the cold-shock protein in the 5th percentile bin in Figure 11. When aligned with their respective thermodynamic profiles, the majority (44/81) of sequences scored better than 99% of the 3858 sequences in the database.

[0037] Figure 12 shows fold-recognition results for 12 all-beta protein targets using a scoring matrix composed of thermodynamic information from 31 all-alpha protein structures. The horizontal axis represents the percentile ranking of the score against the target structure for the sequence corresponding to the target structure. For example, the sequence corresponding to the all-beta target tendamistat (PDB 1hoe) received the 26<sup>th</sup> highest score of 3858 sequences against the tendamistat thermodynamic profile. This result placed the tendamistat sequence in the 5<sup>th</sup> percentile bin in Figure 5. All 12 sequences corresponding to beta targets scored better against their respective targets than 90% of the 3858 sequences in the database.

### DETAILED DESCRIPTION OF THE INVENTION

[0038] It is readily apparent to one skilled in the art that various embodiments and modifications may be made to the invention disclosed in this Application without departing from the scope and spirit of the invention.

[0039] As used herein the specification, "a" or "an" may mean one or more. As used herein in the claim(s), when used in conjunction with the word "comprising", the words "a" or "an" may mean one or more than one. As used herein "another" may mean at least a second or more.

[0040] The term "conformation" as used herein refers various nonsuperimposable three-dimensional arrangements of atoms that are interconvertible without breaking covalent bonds.

[0041] The term "configuration" as used herein refers to different conformations of a protein molecule that have the same chirality of atoms.

[0042] The term "database" as used herein refers to a collection of data arranged for ease of retrieval by a computer. Data is also stored in a manner where it is easily compared to existing data sets.

[0043] The term "enthalpy" as used herein refers to a thermodynamic state or environment in which the enthalpy of internal interactions and the hydrophobic entropy change the favor of protein folding, thus enthalpy is a thermodynamic component in the thermodynamic stability of globular proteins. Enthalpy is a ratio of polar and apolar

contributions ( 
$$H_{ratio,j} = \frac{\Delta H_{pol,j}}{\Delta H_{apol,j}}$$
 ).

[0044] The term "entropy" as used herein refers to a thermodynamic state or environment in which the conformation entropy change works against folding of proteins. Entropy is a ratio the conformational entropy to total solvation free energy

$$(S_{ratio,j} = \frac{\Delta S_{conf,j}}{\Delta G_{solv,j}}).$$

[0045] The term "globular protein" as used herein refers to proteins in which their polypeptide chains are folded into compact structures. The compact structures are unlike the extended filamentous forms of fibrous proteins. A skilled artisan realizes that globular proteins have tertiary structures which comprises the secondary structure elements, e.g., helices,  $\beta$  sheets, or nonregular regions folded in specific arrangements. An example of a globular protein includes, but is not limited to myoglobin.

[0046] The term "peptide" as used herein refers to a chain of amino acids with a defined sequence whose physical properties are those expected from the sum of its amino acid residues and there is no fixed three-dimensional structure.

[0047] The term "polyamino acids" as used herein refers to random sequences of varying lengths generally resulting from nonspecific polymerization of one or more amino acids.

[0048] The term "protein" as used herein refers to a chain of amino acids usually of defined sequence and length and three dimensional structure. The polymerization reaction, which produces a protein, results in the loss of one molecule of water from each amino acid, proteins are often said to be composed of amino acid residues. Natural protein molecules may contain as many as 20 different types of amino acid residues, each of which contains a distinctive side chain.

[0049] The term "protein fold" as used herein refers to an organization of a protein to form a structure which constrains individual amino acids to a specific location relative to the other amino acids in the sequence. One of skill in the art realizes that this type of organization of a protein comprises secondary, tertiary and quarternary structures.

[0050] The term "thermodynamic environment" as used herein refers to the various thermodynamic components that contribute to the folding process of a protein. For example, stability, entropy and enthalpy thermodynamic environments contribute to the folding of a protein. One skilled in the art realizes that the terms "thermodynamic environment", "thermodynamic classification" or "thermodynamic component" are interchangeable.

There is a hierarchy of protein structure. The primary structure is the [0051] covalent structure, which comprises the particular sequence of amino acid residues in a protein and any posttranslational covalent modifications that may occur. The secondary structure is the local conformation of the polypeptide backbone. The helices, sheets, and turns of a protein's secondary structure pack together to produce the three-dimensional The three-dimensional structure of many proteins may be structure of the protein. characterized as having internal surfaces (directed away from the aqueous environment in which the protein is normally found) and external surfaces (which are in close proximity to the aqueous environment). Through the study of many natural proteins, researchers have discovered that hydrophobic residues (such as tryptophan, phenylalanine, tyrosine, leucine, isoleucine, valine or methionine) are most frequently found on the internal surface of protein In contrast, hydrophilic residues (such as asparate, asparagine, glutamate, molecules. glutamine, lysine, arginine, histidine, serine, threonine, glycine, and proline) are most frequently found on the external protein surface. The amino acids alanine, glycine, serine and threonine are encountered with equal frequency on both the internal and external protein surfaces.

25112195.1

[0052] An embodiment of the present invention is a protein database comprising nonhomologous proteins having known residue-specific free energies of folding of the proteins.

[0053] One of skill in the art is cognizant that the properties of proteins are governed by their potential energy surfaces. Proteins exist in a dynamic equilibrium between a folded, ordered state and an unfolded, disordered state. This equilibrium in part reflects the interactions between the side chains of amino acid residues, which tend to stabilize the protein's structure, and, on the other hand, those thermodynamic forces which tend to promote the randomization of the molecule.

[0054] The present invention utilizes a computational method comprising the step of determining a stability constant from the ratio of the summed probability of all states in the ensemble in which a residue j is in a folded conformation to the summed probability of all states in which j is in an unfolded conformation according the equation,

$$K_{f,j} = \frac{\sum P_{f,j}}{\sum P_{nf,j}}$$

[0055] One of skill in the art is cognizant that although the stability constant is defined for each position, the value obtained at each residue is not the energetic contribution of that residue. The stability constant is a property of the ensemble as a whole. For each partially unfolded microstate, the energy difference between it and the fully folded reference state is determined by the energetic contributions of all amino acids comprising the folding units that are unfolded in each microstate, plus the energetic contributions associated with exposing additional (complimentary) surface area on the protein (Figure 1B). The stability constant thus provides the average thermodynamic environment of each residue, wherein surface area, polarity, and packing are implicitly considered. Thus, the stability constant provides a thermodynamic metric wherein each of these static structural properties is weighted according to its energetic impact at each position.

[0056] The stability constants for the residues are arranged into three classifications of stability selected from the group consisting of high, medium and low. Specifically, the residues in the high stability classification comprises phenylalanine, tryptophan and tyrosine. The residues in the low stability classification comprises glycine

13

25112195.1

and proline. The residues in the medium stability classification comprises asparagine and glutamic acid.

In the present invention, the classifications of high, medium and low are determined based upon inspection of the lnkf value for each protein in the selected database. Thus, one of skill in the art is cognizant that these classifications are relative and may vary depending upon the proteins that are selected for the database. One of skill in the art recognizes that these classifications can be subclassified by a variety of other parameters, for example, but not limited to enthalpy and entropy. Thus, any given position in a structure may be represented by two or more parameters, for example, but not limited to low stability (lnkf) and high enthalpy. Yet further, additional parameters can be used to further divide the categories of enthalpy and entropy, for example, but not limited to conformational entropy, solvent entropy, polar enthalpy, apolar enthalpy, polar entropy or apolar entropy. Thus, any given position in a structure may have a description such as, but not limited to low stability, high apolar enthalpy, high polar enthalpy, medium conformational entropy and high apolar entropy. One of skill in the art realizes that these classifications allow for better resolution and consequently, better performance in identifying the correct protein fold for a given protein sequence or a portion of a given protein sequence. Further one of skill in the art is cognizant a protein fold refers to the secondary structure of the protein, which includes sheets, helices and turns.

[0058] Another specific embodiment of the present invention comprises that the stability constants for the residues are arranged into at least one of the three thermodynamic classification groups selected from the group consisting of stability, enthalpy, and entropy.

[0059] Specific embodiments of the present invention provide that the database comprises globular and nonhomologous proteins. A skilled artisan is cognizant that globular proteins are used to study protein folding. It is contemplated that the computational method of the present invention may be used for a variety of globular proteins including but not limiting to glutacorticoid receptor like DNA binding domain, histone, acyl carrier protein like, anti LPS facto/RecA domain, lambda repressor like DNA binding domains, EF hand like, insulin like bacterial Ig/albumin binding, barrel sandwich hybrid, p-loop containing NTP hydrolases, RING finger domain C3HC4, crambin like, ribosomal protein L7/12 C-terminal fragment, cytochrome c, SAM domain like, KH domain, RNA polymerase subunit H, betagrasp (ubiquitin-like), rubredoxin like, HiPiP, anaphylotoxins (complement system),

14

ferrodoxin like, OB fold, midkine, HMG box, saposin, HPr proteins, knottins, HIV-1 Nef protein fragments, thermostable subdomain from chicken villin, SIS/NS1 RNA binding domain, SH3 like barrel, DNA topoisomerase I domain, IL8 like, de novo designed single chain 3 helix bundle, alpha amylase inhibitor tendamistat, CI2 family of serine protease inhibitors protease inhibitors, protozoan pheromone proteins, ConA like lectins/glucoanases, ovomucoid/PCI-1 like inhibitors, beta clip, snake toxin like and BPTI like. Other globular proteins may be selected from the Protein Data Bank.

[0060] One of skill in the art also recognizes that the present invention is not limited to small molecular proteins. A skilled artisan is cognizant that the computational method used in the present invention can be used on larger proteins. Thus, there is not a size limit to the proteins that can be used in the present invention.

[0061] Another embodiment of the present invention is a method of developing a protein database comprising the steps of: inputting high resolution structures of proteins; generating an ensemble of incrementally different conformations by combinatorial unfolding of a set of predefined folding units in all possible combinations of each protein; determining the probability of each said conformational state; calculating the residue-specific free energy of each conformational state; and classifying a stability constant into at least one thermodynamic environment selected from the group consisting of stability, enthalpy, and entropy.

[0062] In specific embodiments, the generating step comprises dividing the proteins into folding units by placing a block of windows over the entire sequence of the protein and sliding the block of windows one residue at a time.

[0063] One of skill in the art is cognizant that the division of a protein into a given number of folding units is a partition. Thus, to maximize the number of partially folded states, different partitions are used in the analysis. The partitions can be defined by placing a block of windows over the entire sequence of the protein. The folding units are defined by the location of the windows irrespective of whether they coincide with specific secondary structure elements. By sliding the entire block of windows one residue at a time, different partitions of the protein are obtained. For two consecutive partitions, the first and last amino acids of each folding unit are shifted by one residue. This procedure is repeated until the entire set of partitions has been exhausted. In specific embodiments, windows of 5

or 8 amino acid residues are used. One of skill in the art realizes that approximately  $10^5$  partially folded conformations can be generated using the COREX algorithm. This value can be altered by increasing or decreasing the window size and the size of the protein. For example, for the proteins  $\lambda 6$ -85, chymotrypsin inhibitor 2 and barnase, windows sizes of 5, 5, 8 and amino acid residues results in  $2.6 \times 10^5$ ,  $0.4 \times 10^5$ , and  $1.1 \times 10^5$  partially folded conformations, respectively.

[0064] In further embodiments, the determining step comprises determining the free energy of each of the conformational states in the ensemble; determining the Boltzmann weight  $[K_i = \exp(-\Delta G_i/RT)]$  of each state; and determining the probability of each state using the equation,

$$P_i = \frac{K_i}{\sum K_i'}$$

[0065] Yet further, the calculating step comprises determining the energy difference between all microscopic states in which a particular residue is folded and all such states in which it is unfolded using the equation,

$$\Delta G_{f,i} = -RT \cdot ln \kappa_{f,i}$$

[0066] One of skill in the art is aware that the COREX algorithm generates a large number of partially folded states of a protein from the high resolution crystallographic or NMR structure (Hilser & Freire, 1996; Hilser & Freire, 1997 and Hilser *et al.*, 1997). In this algorithm, the high resolution structure is used as a template to approximate the ensemble of partially folded states of a protein. Thus, the protein is considered to be composed of different folding units. The partially folded states are generated by folding and unfolding these units in all possible combinations. There are two basic assumptions in the COREX algorithm: (1) the folded regions in partially folded states are native-like; and (2) the unfolded regions are assumed to be devoid of structure or lacking structure. Thermodynamic quantities, *e.g.*,  $\Delta H$ ,  $\Delta S$ ,  $\Delta Cp$ , and  $\Delta G$ , partition function and probability of each state ( $P_i$ ) are evaluated using an empirical parameterization of the energetics (Murphy & Freire, 1992; Gomez *et al.*, 1995; Hilser *et al.*, 1996; Lee *et al.*, 1994; D'Aquino *et al.*, 1996; and Luque *et al.*, 1996).

16

[0067] Yet further, a skilled artisan is cognizant that the residue specific equilibrium provide quantitative agreement with those obtained experimentally from amide hydrogen exchange experiments, *e.g.*, hydrogen protection factors (Hilser & Freire, 1996; Hilser & Freire, 1997; and Hilser *et al.*, 1997).

[0068] One of skill in the art realizes that while the residue stability constants are purely thermodynamic quantities defined for all residues, the protection factors also contain non-thermodynamic contributions and are defined for a subset of residues.

[0069] Another embodiment of the present invention is a method of identifying a protein fold comprising determining the distribution of amino acid residues in different thermodynamic environments corresponding to a known protein structure. More particularly, determining the distribution of amino acid residues comprises constructing scoring matrices derived of thermodynamic information. Specifically, the scoring matrices are derived from COREX thermodynamic information, such as stability, enthalpy, and entropy. Thus, COREX-derived thermodynamic descriptors can be used to identify sequences that correspond to a specific fold.

[0070] A skilled artisan recognizes that the COREX algorithm provides a means of estimating the energetic variability in the native state of proteins, and uses this information to illuminate the relation between amino acid sequence and protein structure. Therefore, the thermodynamic information obtained by the COREX algorithm represents a fundamental descriptor of proteins that transcends secondary structure classifications.

[0071] Protein folds can be considered as one of the most basic molecular parts. A skilled artisan recognizes that the properties related to protein folds can be divided into two parts, intrinsic and extrinsic. The intrinsic properties relates to an individual fold, e.g., its sequence, three-dimensional structure and function. Extrinsic properties relates to a fold in the context of all other folds, e.g., its occurrence in many genomes and expression level in relation to that for other folds.

[0072] Further, one of skill in the art realizes that other methods well known in the art can be used to develop protein databases for example, but not limited to Monte Carlo sampling method. The Monte Carlo sampling method is well known and used in the art (Pan et al., 2000).

#### **EXAMPLES**

[0073] The following examples are included to demonstrate preferred embodiments of the invention. It should be appreciated by those skilled in the art that the techniques disclosed in the examples which follow represent techniques discovered by the inventor to function well in the practice of the invention, and thus can be considered to constitute preferred modes for its practice. However, those of skill in the art should, in light of the present disclosure, appreciate that many changes can be made in the specific embodiments which are disclosed and still obtain a like or similar result without departing from the concept, spirit and scope of the invention.

### **Example 1 Selection of proteins used in dataset**

[0074] A database of 44 proteins, 2922 residues total (Table 1), was selected from the Protein Data Bank on the basis of biological and computational criteria. The two biological criteria were that the proteins be globular and nonhomologous with every other member of the set as ascertained by SCOP (Murzin et al., 1995). The first computational criterion was that the proteins be small (less than about 90 residues), because the CPU time and data storage needs of an exhaustive COREX calculation increased exponentially with the chain length. The second computational criterion was that the structures be mostly devoid of ligands, metals, or cofactors, as the COREX energy function was not parameterized to account for the energetic contributions of non-protein atoms. The database was comprised of 24 x-ray structures, whose resolution ranged from 2.60 to 1.00 Å (median value of 1.65 Å). Twenty NMR structures completed the database. An independent database of 50 proteins (3304 residues total) that were not included in the above set, was created from the PDBSelect database (Hobohm & Sander, 1996). This second database was used as a control to check the results obtained from the first database, as shown in Figure 7.

## 

Table 1. SCOP Classifications and Sequence Data for 44 Proteins Used in the Database

NUMBER	PDB ID	PDB LENGTH <sup>A</sup>	SCOP FOLD <sup>B</sup>	SEQUENCE LENGTH <sup>c</sup>	NUMBER OF SEQUENCES <sup>D</sup>
1	1a7I	09	Glutacorticoid receptor like DNA binding domain	81	20
2	la7w	89	Histone	69	17
3	1a8o	02	Acyl carrier protein like	20	22
4	1aa3	63	Anti LPS factor / RecA domain	63	12
5	1adr	92	Lambda repressor like DNA binding domains	92	35
9	1ak8	92	EF hand like	92	35
7	1b9g	57	Insulin like	57	12
8	1bdd	09	Bacterial Ig / albumin binding	09	32
6	1bdo	80	Barrel sandwich hybrid	80	14
10	1c1y	27	P-loop containing NTP hydrolases	77	25
11	1chc	89	RING finger domain C3HC4	89	21
12	lcnr	46	Crambin like	46	30
13	1ctf	89	Ribosomal protein L7/12 C-terminal fragment	74	14
14	1ctj	89	Cytochrome c	68	17
15	1doq	69	SAM domain like	69	17
16	1dt4	73	KH domain	73	16
17	1hmj	89	RNA polymerase subunit H	78	8
18	ligd	61	Beta-grasp (ubiquitin-like)	61	12
19	liro	53	Rubredoxin like	54	16
20	1isu	62	HiPiP	62	30
21	1kjs	74	Anaphylotoxins (complement system)	74	14
22	1kp6	62	Ferrodoxin like	62	24
23	1mjc	69	OB fold	69	17

## 

							,														
6	20	8	33	19	12	20	6	23	25	25	16	14	8	24	17	9	25	31	30	23	
59	81	78	87	64	57	29	59	58	22	71	73	74	83	40	75	52	99	99	62	58	
Midkine	HMG box	Saposin	HPr proteins	Knottins	HIV-1 Nef protein fragments	Thermostable subdomain from chicken villin	SIS / NS1 RNA binding domain	SH3 like barrel	DNA topoisomerase I domain	IL8 like	De novo designed single chain 3 helix bundle	Alpha amylase inhibitor tendamistat	CI2 family of serine protease inhibitors	Protozoan pheromone proteins	DNA / RNA binding 3-helical bundle	Con like lectins / glucanases	Ovomucoid / PCI-1 like inhibitors	Beta clip	Snake toxin like	BPTI like	ממת ו
59	62	78	87	64	95	29	56	58	77	71	73	74	65	\$	65	47	56	99	62	56	1.7
1mkn	Inhm	1nkl	1ptf	lptx	1qa4	lqqv	1r1b	1sem	1vcc	lvmp	2a3d	2ait	2ci2	2erl	2ezh	21al	2ovo	2spg	3ebx	6pti	
24	25	26	27	28	29	30	31	32	33	34	35	36	37	38	39	40	41	42	43	44	

<sup>a</sup> The number of residues for which coordinates are reported in the PDB entry.

<sup>b</sup> The structural classification for determining extent of homology as found in the SCOP database (Murzin et al., 1995).

<sup>c</sup> The number of residues in the entire amino acid sequence as given in the PDB entry. All amino acid sequences contained in the foldrecognition library of a given target structure were of this length.

<sup>d</sup> The number of amino acid sequences contained in the fold-recognition library of a given target structure and represents the total number of monomeric sequences in the PDB with lengths identical to the value in the "Sequence Length" column.

### Example 2 Computational Details

[0075] The database of 44 nonhomologous proteins (Table 1) was analyzed using the COREX algorithm. The COREX algorithm (Hilser & Freire, 1996) was run with a window size of five residues on each protein in the database. The minimum window size was set to four, and the simulated temperature was 25 °C.

[0076] Briefly, COREX generated an ensemble of partially unfolded microstates using the high-resolution structure of each protein as a template (Hilser & Freire, 1996). This was facilitated by combinatorially unfolding a predefined set of folding units (i.e., residues 1 - 5 are in the first folding unit, residues 6-10 are in the second folding unit, etc.). By means of an incremental shift in the boundaries of the folding units, an exhaustive enumeration of the partially unfolded species was achieved for a given folding unit size. The entire procedure is shown schematically in Figure 1A for ovomucoid third domain (OM3), one of the proteins in the database (PDB accession code 20vo).

[0077] For each microstate i in the ensemble, the Gibbs free energy was calculated from the surface area-based parameterization described previously (D'Aquino, 1996; Gomez, 1995; Xie, 1994; Baldwin, 1986; Lee, 1994; Habermann, 1996). The Boltzmann weight of each microstate [i.e.,  $Ki = \exp(-\Delta G_i/RT)$ ] was used to calculate its probability:

$$P_i = \frac{K_i}{\sum K_i} \tag{1}$$

[0078] where the summation in the denominator is over all microstates. From the probabilities calculated in Equation 1, an important statistical descriptor of the equilibrium was evaluated for each residue in the protein. Defined as the residue stability constant,  $\kappa_{f,j}$ , this quantity was the ratio of the summed probability of all states in the ensemble in which a particular residue j was in a folded conformation  $(\Sigma P_{nf,j})$ :

$$\kappa_{f,j} = \frac{\sum P_{f,j}}{\sum P_{nf,j}} \tag{2}$$

[0079] From the stability constant, a residue-specific free energy was written as:

$$\Delta G_{f,j} = -RT \cdot ln\kappa_{f,j} \tag{3}$$

[0080] Equation 3 reflects the energy difference between all microscopic states in which a particular residue was folded and all such states in which it is unfolded.

[0081] The Gibbs energy for each microstate i relative to the fully folded structure was calculated using Equation 4:

$$\Delta Gi = \Delta Hi$$
, solvation  $-T(\Delta Si$ , solvation  $+ W\Delta Si$ , conformational) (4)

[0082] where the calorimetric enthalpy and entropy of solvation were parameterized from polar and apolar surface exposure, and the conformational entropy was determined as described previously (Hilser & Freire, 1996). The maximum stability for each protein was normalized to a common arbitrary value of approximately 6.2 kcal/mol (max  $\ln \kappa_f = 10.4$ ) by adjusting its conformational entropy factor, W, in Equation 4. The average entropy factor required for the normalization was  $0.81 \pm 0.19$  (mean  $\pm$  s.d.) over the 44 proteins. It was an empirical observation that adjustment of a stable protein's conformational entropy factor did not change the relative patterns of high and low stability regions in the structure.

## Example 3 Comparison of Residue Stability Constant to Hydrogen Exchange Protection Factors

[0083] Prediction of the hydrogen exchange protection factors of the residues that exchange protons was performed by calculation of the ensemble of  $P_{f,i}$  and  $P_{f,cx,j}$  values.

[0084] Briefly, the protection factor for any given residue j was defined as the ratio of the sum of the probabilities of the states in which residue j was closed, to the sum of the probabilities of the states in which residue j was open:

$$PF_{j} = \frac{\sum P_{i}}{\sum P_{i}} = \frac{P_{\text{closed }, j}}{P_{\text{open }, j}}$$
(5)

[0085] The statistical definition of the protection factors has the same form as that of the stability constants (equation (2)) and was expressed in terms of the folding probabilities as follows:

$$PF_{j} = \frac{P_{f, j} - P_{f, xc, j}}{P_{n, f, j} + P_{f, xc, j}}$$
(6)

[0086] The correction term  $P_{f,xc,j}$  was the sum of the probabilities of all states in which residue j was folded, yet exchange competent.

[0087] Figure 2 shows the comparison of hydrogen exchange protection factors predicted from COREX data with experimental values for OM3. The agreement in the location and relative magnitude of the protection factors with the stability constants for this and other proteins suggested that the calculated native state ensemble provided a good description of the actual ensemble (Hilser & Freire, 1996). It naturally follows that the residue stability constants of a particular protein provided a good description of the thermodynamic environment of each residue in that structure.

[0088] Further inspection of Figure 2 revealed another important feature in the pattern of residue stability constants. Namely, the stability constants varied significantly across a given secondary structural element, as observed for alpha helix 1 of OM3. The protection factors (and stability constants) were high at the N-terminal region of helix 1, but decreased over the length of the helix. This indicated that secondary structure, or other structural classifications, do not obligatorily coincide with thermodynamic classifications. This result has potentially important consequences for cataloging propensities of amino acids in different environments. For example, in OM3 two threonine residues were located in different structural environments; Thr 47 was part of the loop that follows alpha helix 1, while Thr 49 was part of beta strand 3. In spite of the different structural environments for the two threonine residues, the stability constants and, more importantly, the experimental protection factors demonstrated that both residues, to a first approximation, share the same thermodynamic environment.

## **Example 4 Binning of Residue Stability Constants**

[0089] Inspection of each protein's  $\ln \kappa_f$  data indicated that these were the three stability classes: high, medium, and low stability. The cutoffs for each stability class were

25112195.1 23

adjusted so that an approximately equal number of residues in the database fell in each class (Table 2). The low stability category was defined as  $\ln \kappa_f \ll 3.99$ , the medium stability category was defined as  $3.99 < \ln \kappa_f \ll 7.14$ , and the high stability category was defined as  $\ln \kappa_f > 7.14$ . Statistics of amino acid type as a function of each of these stability categories were tabulated (Table 2), and normalized histograms of these numbers are shown in Figure 3A-Figure 3T.

Table 2. Statistics of  $ln \kappa_f V$  alues for 2922 Residues in the Database<sup>a</sup>

Table 2. S		Values for 2922 Re		
Residue	Low	Medium	High	Row
Type	$(\ln \kappa_f < =$	$(3.99 < \ln \kappa_f)$	(7.14 <	Total
	3.99)	<= 7.14)	lnk <sub>f</sub> )	
Ala	95	88	91	274
Arg	33	43	63	139
Asn	46	47	33	126
Asp	42	69	45	156
Cys	36	34	51	121
Gln	22	34	51	107
Glu	68	86	70	224
Gly	125	71	25	221
His	20	10	14	44
Ile	36	55	54	145
Leu	· 58	70	87	215
Lys	99	78	61	238
Met	20	19	18	57
Phe	11	23	62	96
Pro	71	41	22	134
Ser	46	41	58	145
Thr	70	51	32	153
Trp	10	5	22	37
Туг	15	27	50	92
Val	48	79	71	198
Column Total	971	971	980	2922

The values in this table were used to compute the normalized histograms shown in Figure 3A-Figure 3T. In addition, these values (minus the values for a given target protein) were used to compute the  $\ln \kappa_f$  scoring matrices.

[0090] Striking asymmetries were often observed for the histograms of certain amino acids across the three stability environments, and these asymmetries were well outside the standard deviation of the average of three random data sets. For example, the aromatic amino acids Phe, Trp, and Tyr were mostly found in high stability environments, while Gly and Pro were overwhelmingly found in low stability environments. In contrast, other

residues such as Ala, Met, and Ser exhibited distributions that did not significantly differ from randomized data.

[0091] Although the acidic residues Asp and Glu shared a slight tendency to be found in medium stability environments, it was observed that several amino acid pairs having nominally similar chemical characteristics partition differently in the stability environments. For example, the basic residues Arg and Lys exhibited opposite stability characteristics: the counts for Arg increased as the stability class increased, but the counts for Lys decreased as a function of stability class. While Asn was found less often in high stability environments, Gln was found more often in them. Although the distribution for Ser did not differ significantly from the randomized data, Thr occurred more often in low stability environments and less often in high stability environments. Somewhat surprisingly, the aliphatic amino acids Ile, Leu, and Val did not show a general pattern, except perhaps a slight disfavoring of low stability environments.

## Example 5 Calculation of Average Native State Side Chain Area Surface Exposure

[0092] Average side chain area surface area exposure of residue j over a window size of five residues, ASA<sub>average,j</sub>, was calculated using Equation 7:

$$ASA_{average,j} = \frac{\sum_{i=j-2}^{i=j+2} ASA_{native,j}}{5}$$
 (7)

[0093] Because Equation 7 was undefined for the first and last two residues in each protein, these four residues were ignored in the binning. The cutoffs for each side chain area class were adjusted so that an approximately equal number of residues fell in each class. The low exposure category was defined as  $ASA_{average,j} \le 43.31 \text{ Å}^2$ , the medium exposure category was defined as  $43.31 \text{ Å}^2 < ASA_{average,j} \le 59.86 \text{ Å}^2$ , and the high exposure category was defined as  $ASA_{average,j} > 59.86 \text{ Å}^2$ .

[0094] As shown in Figure 4, frequencies of amino acids found in COREX stability environments were not correlated to frequencies of amino acids in exposed surface area environments. This was important as it suggested that the thermodynamic information calculated by the COREX algorithm was not simply monitoring a static property of the structure, but instead was capturing a property of the native state ensemble as a whole.

### Example 6 Random DataSets

[0095] For comparison to the COREX and DSSP data sets from the 44 non-homologous proteins in the database, control data sets were constructed by randomizing (i.e., shuffling) the calculated stability and the secondary structure data. The random data sets therefore contained the same amino acid composition, counts of high, medium, and low stabilities, and types of secondary structure, as the real data sets. However, any correlation between residue type or secondary structural class was presumably destroyed by randomization. To assess internal variability of the data due to differing numbers of counts of each residue type, the results from three randomized data sets were averaged and standard deviations calculated; these data are plotted in Figure 3A-Figure 3T.

## Example 7 Construction of Scoring Matrices

[0096] The scoring matrices were calculated as log-odds probabilities of finding residue type j in structural environment k, as described below and in (Bowie *et al.*, 1991). The matrix score,  $S_{j,k}$ , was defined as:

$$S_{j,k} = \ln \frac{P_j \mid k}{P_k} \tag{8}$$

[0097] In Equation 8,  $P_j \mid k$  was the probability of finding a residue of type j in stability class k (i.e., number of counts of residue type j), and  $P_k$  was the probability of finding any residue in the database in stability environment k (i.e., number of residues in stability class k, regardless of amino acid type, divided by the total number of residues in the entire database, regardless of amino acid type). The structural environment was described by either COREX stability information (high, medium, or low  $ln\kappa_j$ ), or DSSP secondary structure (alpha, beta, or other) as given in the target's PDB entry. The fold recognition target was removed from the database, and the remaining 43 proteins were used to calculate the scores; therefore, information about the target was never included in the scoring matrix. The values in Tables 3A and 3B are the average  $\pm$  standard deviation of all 44 individual scoring matrices.

Table 3. Average 3D-1D Scoring Matrices Derived from  $\ln \kappa_f$  and Secondary Structure Information<sup>a</sup>

4

			-				,	•	(	۶
	M	T.	Y	<u> </u>	I	>	Σ	V	C	P
Low	-0.21	-1.06	-0.71	-0.21	-0.29	-0.32	0.05	0.04	0.53	0.47
\$	+0.05	±0.04	+0.04	±0.02	±0.02	±0.05	±0.03	±0.02	±0.01	±0.01
Medium	-0.90	-0.33	-0.12	-0.02	0.13	0.18	0.00	-0.03	-0.03	-0.08
Modulii	+0.06	+0.02	±0.03	±0.01	±0.01	±0.01	±0.03	±0.01	±0.02	±0.02
High	0.57	0.66	0.48	0.19	0.10	0.07	90.0	-0.01	-1.09	-0.71
ııgıı	+0.02	±0.01	±0.02	±0.01	±0.01	±0.01	±0.05	±0.01	±0.03	±0.03

	C	L	S	0	Z	王	D	Н	K	R
I ow	-0.11	0.32	-0.05	-0.48	0.00	-0.09	-0.21	0.31	0.22	-0.34
¥	±0.02	±0.01	±0.02	±0.03	±0.02	±0.01	±0.05	±0.03	±0.02	±0.03
Medium	-0.17	0.00	-0.16	-0.04	0.12	0.14	0.29	-0.38	-0.01	-0.07
INTOGRATI	+0.03	±0.05	±0.02	±0.02	±0.02	±0.01	±0.01	±0.04	±0.02	±0.02
High	0.23	-0.47	0.18	0.35	-0.25	-0.07	-0.15	-0.05	-0.27	0.30
111811	±0.02	±0.03	±0.01	±0.02	±0.03	±0.01	±0.02	±0.04	±0.02	±0.05

m M

	M	[Ti	Y	T		Λ	M	A	G	Ь
Alnhac	-0.20	0.04	-0.04	0.30	0.11	-0.22	0.16	0.42	-0.85	-1.08
pudiv,	±0.04	±0.03	±0.03	±0.01	±0.02	±0.02	±0.03	±0.01	±0.03	±0.03
Reta	0.57	0.78	99.0	-0.22	0.52	19.0	-0.31	-0.65	-0.44	-0.47
<b>1</b>	+0.0+	±0.02	±0.03	±0.03	±0.02	±0.02	≠0.06	±0.03	±0.03	±0.04
Other	-0.15	-0.55	-0.34	-0.17	-0.36	-0.21	-0.02	-0.20	0.40	0.44
	±0.03	±0.03	±0.02	±0.01	±0.03	±0.05	±0.02	±0.02	±0.01	±0.01

# 

										_
						F	_		<u> </u>	~
	ر	<u>-</u>	V.		Z	T)	ח	<u></u>	4	11
	ر	٦_	2	<b>Y</b>				l	213	010
			, 00	100	270	750				0.1 <i>y</i>
A 1 1.	700	_0 57	77	C.5.0	-0.03	65.0				
Albha	20.02	10.0		)					+0.01	1 +0.02
myrdfre r	,	2000	70 07	+0.02	+0.03	10.01	±0.02	TO:01	10:0∓	
	10.03	c0.0±	TO.02	70:0∓		9.			77	- 11
	000	7 1 0		000	070	-0 4d			-C.O.	-N.11
D.42	×	77	07.0-	07.0	\r.o.					
Sela	00.0		1		,				+0.03	+0.03
			±0.03	+0.02	+0.03	140.03			70.05	
	+0.04	±0.02	CO.01	70:07			l		700	- 11
				0.43	75 0	7 C			cn.n	1-0-
0.15.2		Y = =	77.0	24.0-	20.0	CT.0_				
TURE	20.0								+0 01	+0.02
	•		100	CU UT	+001	10.01			70.01	=2:0=
	20 O+ I	10.01	±0.01	1 TO:02	10:01				1 1	tuodo moitoum

Each of the 44 targets used in the fold-recognition experiments had an individual 3D-1D scoring matrix that did not include information about <sup>b</sup> The boundaries for the stability categories were defined as follows: low stability was  $\ln \kappa_f <= 3.99$ , medium stability was  $3.99 < \ln \Box_f <= 7.14$ , the target. Consequently, matrix scores are reported as the average (large bold numbers) ± standard deviation (small numbers) of 44 values.

<sup>c</sup> DSSP secondary structure (Kabsch & Sander, 1983) was used as given in each protein's PDB entry. high stability was  $7.14 < \ln \kappa_f$ , as described in the text.

[0098] The scoring matrices derived from COREX stability and secondary structure, averaged over all 44 target proteins, are shown in Tables 3A and 3B, respectively. The stability matrix scores faithfully reflected the histograms shown in Figure 3A-Figure 3T; for example, Gly and Pro scored unfavorably in high stability environments but scored favorably in low stability environments. Similarly, the secondary structure matrix scores followed intuitive notions of secondary structure propensity; for example, Ala scored positively in helical environments, the aromatics scored positively in beta environments, and Gly and Pro scored negatively in both alpha and beta environments. The standard deviations in both matrices were generally small as compared to the magnitude of the scores, suggesting that the scores were not affected by the removal of any one protein from the database.

### **Example 8 Fold-Recognition Details**

[0099] Fold-recognition experiments were based on the profile method pioneered by Eisenberg and co-workers (Gribskov *et al.*, 1987; Bowie *et al.*, 1991).

[0100] Briefly, the method characterized each residue position of a target protein in terms of a structural environment score derived from analysis of a database of known structures. The resulting profile of the target protein was then optimally aligned to each member of a library of amino acid sequences by maximizing the score between the sequence and the profile. Two structural environment scoring schemes were developed: one based on calculated COREX stability, and one based on DSSP secondary structure (Kabsch & Sander, 1983) as contained in each target protein's PDB file. Each scoring scheme had three dimensions as a function of the 20 amino acids: high, medium, and low stability for COREX scoring, or alpha, beta, and other for secondary structure scoring. Two alignment algorithms were used: a local scheme (Smith & Waterman, 1981) as implemented in the PROFILESEARCH software package (Bowie et al., 1991), and a global scheme. The global alignment scheme simply paired the first residue of an amino acid sequence with the first position of a target profile, with no allowance for gaps. This scheme was possible because the amino acid sequence lists against which the targets were threaded only included sequences of identical length to each target corresponding to monomeric structures from the PDB. The total number of identical length sequences for each target ranged from 6 to 35, with an average of  $19 \pm 8$  sequences per target (Table 1). No attempt was made to optimize 25112195.1 29

the gap opening and extension penalties for the local algorithm; in all cases these were the defaults given in the PROFILESEARCH package, 0.1 and 0.05, respectively.

[0101] The results of the fold recognition experiments are shown in Figure 5A, Figure 5B, Figure 5C and Figure 5D, and at least three conclusions are drawn from this data. First, scoring matrices composed of either COREX stability or DSSP secondary structure data performed better than randomized data sets in matching a structural target to its amino acid sequence. In Figure 5A, Figure 5B, Figure 5C and Figure 5D, the results for COREX data are stacked toward the left (successful) side of the rankings, while the randomized data approaches a bell-shaped distribution with a maximum near the median of the size of the sequence datasets (approximately 10 for the mean size of 19 sequences). Second, for both COREX and DSSP scoring matrices, the global algorithm (which took the entire amino acid sequence into account) performed significantly better than the local algorithm (which generally aligned only a subset of the sequence). Third, the total number of targets falling in the most successful bin was similar for both the COREX stability and secondary structure matrices, suggesting that COREX stability propensities alone contained a comparable amount of information to secondary structure propensities.

[0102] Because the local alignment algorithms used here compute a score without returning the complete alignment of profile to sequence, high scores may have been possible from non-structurally significant local alignments. In other words, it is possible that a correct sequence may have scored well against its corresponding target structure without having placed the individual amino acids in their correct positions within the structure. The use of the global alignment in conjunction with amino acid sequences of identical length partially alleviated this problem, as no misalignment was allowed in the global scheme.

## **Example 9 Successful Alignment Based on COREX Stability**

[0103] To assess the extent of local alignments that were structurally significant, minor modifications were made to the PROFILESEARCH source code that saved the traceback of the alignment matrix. It was found that for targets scoring poorly in the fold-recognition rankings, local alignments of the corresponding sequence were often not significant. However, sequences that scored in the top two bins were often found to be

25112195.1

completely and correctly aligned with their target profiles, even though not all of their residues contributed to the overall score due to the rules of the local algorithm. Three examples of successful alignment based on COREX stability data alone are shown in Figures 6A, 6B, 6C and Tables 4A, 4B, 4C for the targets Protein G (1igd), DNA topoisomerase I (1vcc), and tendamistat (2ait), respectively. The alignments calculated using the local algorithm were correct, despite the fact that no sequence information about the target was used, and that only a subset of the amino acid sequence was used in the scoring. In addition, it is noteworthy that the success of these examples is not due to merely a small fragment of the sequence, as the cumulative 3D-1D matrix score steadily increase over the entire length of the sequence.

Table 4A. Local Alignment Score of 1igd Sequence to 1igd Stability Profile

Residue	Residue	Stability	3D-1D	Cumulative
Number	Type*	<b>Environment</b> <sup>a</sup>	Matrix	Local
			Scoreb	Alignment
				Score <sup>c,d</sup>
1	M	L	0.02	0.02
2	T	L	0.30	0.32
3	P	L	0.46	0.78
4	A	·L	0.05	0.83
5	V	L	-0.33	0.50
6	T	L	0.30	0.80
7	T	L	0.30	1.10
8	Y	M	-0.13	0.97
9	K	Н	-0.29	0.68
10	L	H	0.19	0.87
11	V	M	0.17	1.04
12	I	M	0.12	1.16
13	N	M	0.10	1.26
14	G	L	0.54	1.80
15	K	L	0.22	2.02
16	Т	L	0.30	2.32
17	L	L	-0.22	2.10
18	K	L	0.22	2.32
19	G	L	0.54	2.86
20	Е	L	-0.09	2.77
21	Т	L	0.30	3.07
22	Т	L	0.30	3.37
23	Т	L	0.30	3.67
24	K	L	0.22	3.89

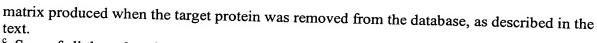
25112195.1

25	A	L	0.05	3.94
26	V	L	-0.33	3.61
27	D	L	-0.20	3.41
28	A	M	-0.03	3.38
29	E	M	0.15	3.53
30	T	M	0.05	3.58
31	A	Н	-0.02	3.56
32	Е	Н	-0.08	3.48
33	K	H	-0.29	3.19
34	A	Н	-0.02	3.17
35	F	Н	0.64	3.81
36	K	Н	-0.29	3.52
37	Q	Н	0.34	3.86
38	Y	Н	0.48	4.34
39	Α	Н	-0.02	4.32
40	N	M	-0.25	4.07
41	D	M	0.26	4.33
42	N	M	0.10	4.43
43	G	M	-0.05	4.38
44	V	M	0.17	4.55
45	D	M	0.26	4.81
46	G	M	-0.05	4.76
47	V	M	0.17	4.93
48	W	Н	0.55	5.48
49	T	Н	-0.52	4.96
50	Y	Н	0.48	5.44
51	D	M	0.26	5.70
52	D	M	0.26	5.96
53	A	M	-0.03	5.93
54	T	M	0.05	5.98
55	K	M	0.00	5.98
56	T	Н	-0.52	5.46
57	F	Н	0.64	6.10
58	T	Н	-0.52	5.58
59	V	Н	0.08	5.66
60	T	Н	-0.52	5.14
61	E	Н	-0.08	5.06
		1 11 D 11-	1 1in	tod by the one lette

<sup>\*</sup>One of skill in the art recognizes that the Residue types are listed by the one letter amino acid designation.

<sup>&</sup>lt;sup>a</sup> H, M, and L denote high, medium, and low stability as defined in the text and in footnote b

Value of the 3D-1D scoring matrix corresponding to the results of optimal alignment of the 1igd amino acid sequence given in the "Residue Type" column to the 1igd stability profile given in the "Stability Environment" column. These values are highly similar, but not identical, to the average values given in Table 3A because these values are from the scoring 32



<sup>c</sup> Sum of all the values in the "3D-1D Matrix Score" column up to and including the indicated residue number. Values in boldface were used by the local alignment algorithm (Smith & Waterman, 1981) to compute the optimal sequence to profile alignment.

d Data in the "Cumulative Local Alignment Score" column was used to generate Figure 5A.

Table 4B. Local Alignment Score of 1vcc Sequence to 1vcc Stability Profile

Residue	Residue	nt Score of 1vcc S Stability	3D-1D	Cumulative
Number	Type*	Environment <sup>a</sup>	Matrix	Local
	- <u>-</u>		Score <sup>b</sup>	Alignment
				Score <sup>c,d</sup>
1	M	Н	0.00	0.00
2	R	H	-0.08	-0.08
3	A	H	0.30	0.22
4	L	H	-0.01	0.21
5	F	H	0.19	0.40
6	Y	M	0.66	1.06
7	K	L	-0.14 0.19	0.92
8	D	L		1.11
9	G	L	-0.25	0.86
10	K	L	0.53 0.19	1.39
11	L			1.58
12	F	M	-0.04	1.54
13	<u>г</u> Т	H M	0.66	2.20
14	D		0.00	2.20
15	N N	M	0.28	2.48
16	N	M	0.06	2.54
17	F	M M	0.06	2.60
18	L		-0.36	2.24
19	N N	M M	-0.04 0.06	2.20
20	P	M	-0.11	2.26
21	V	M		2.15
22	S	M	0.19	2.34
23	D	M	-0.19	2.15
24	$\frac{D}{D}$	M	0.28	2.43
25	N		0.28	2.71
26	P	M M	0.06	2.77
27	A		-0.11	2.66
28	<u>- А</u>	M H	-0.04 0.50	2.62
29	E	M M	-0.10	3.12
30	V	M	0.10	3.02
31	L	M		3.21
32	Q	M	-0.04	3.17
33	H		-0.04 0.22	3.13
34	V	L L	-0.32	3.35
35	K	L	0.19	3.03
36	I	L		3.22
37	P		-0.31	2.91
38	T	L L	0.47	3.38
	1	L	0.32	3.70

39	Н	L	0.22	3.92
40	L	L	-0.19	3.73
41	T	L	0.32	4.05
42	D	L	-0.25	3.80
43	V	M	0.19	3.99
44	V	Н	0.06	4.05
45	V	Н	0.06	4.11
46	Y	H	0.50	4.61
47	Е	Н	-0.10	4.51
48	Q	Н	0.34	4.85
49	T	Н	-0.47	4.38
50	W	Н	0.55	4.93
51	Е	Н	-0.10	4.83
52	Е	М	0.15	4.98
53	A	М	-0.04	4.94
54	L	M	-0.04	4.90
55	T	M	0.00	4.90
56	R	М	-0.06	4.84
57	L	Н	0.19	5.03
58	Ī	Н	0.10	5.13
59	F	Н	0.66	5.79
60	V	Н	0.06	5.85
61	G	Н	-1.11	4.74
62	S	M	-0.19	4.55
63	D	L	-0.25	4.30
64	S	L	-0.05	4.25
65	K	L	0.19	4.44
66	G	L	0.53	4.97
67	R	L	-0.34	4.63
68	R	H	0.30	4.93
69	Q	H	0.34	5.27
70	Y	M	-0.14	5.13
71	F	M	-0.36	4.77
72	Y	L	-0.73	4.04
12	<u> </u>	<u> </u>		

35

73	G	L	0.53	4.57
74	K	L	0.19	4.76
75	M	L	0.04	4.80
76	Н	L	0.22	5.02
77	V	L	-0.32	4.70

<sup>\*</sup> One of skill in the art recognizes that the Residue types are listed by the one letter amino acid designation.

Data in the "Cumulative Local Alignment Score" column was used to generate Figure 5B.

<sup>&</sup>lt;sup>a</sup> H, M, and L denote high, medium, and low stability as defined in the text and in footnote b of Table 3.

<sup>&</sup>lt;sup>b</sup> Value of the 3D-1D scoring matrix corresponding to the results of optimal alignment of the 1vcc amino acid sequence given in the "Residue Type" column to the 1igd stability profile given in the "Stability Environment" column. These values are highly similar, but not identical, to the average values given in Table 3A because these values are from the scoring matrix produced when the target protein was removed from the database, as described in the

<sup>&</sup>lt;sup>c</sup> Sum of all the values in the "3D-1D Matrix Score" column up to and including the indicated residue number. Values in boldface were used by the local alignment algorithm (Smith & Waterman, 1981) to compute the optimal sequence to profile alignment.

Table 4C. Local Alignment Score of 2ait Sequence to 2ait Stability Profile

Residue Number	Residue Type*	Stability Environment	3D-1D Matrix Score <sup>b</sup>	Cumulative Local Alignment Score <sup>c,d</sup>
	NI NI	L	-0.21	-0.21
11	N T	L	0.31	0.1
2	T	L	0.31	0.41
3	V	L	-0.3	0.11
4	S	L	-0.06	0.05
5	E	L	-0.11	-0.06
6	P	L	0.47	0.41
7 8	A	M	-0.04	0.37
9	$\frac{A}{P}$	M	-0.1	0.27
10	S	M	-0.14	0.13
11	$\frac{1}{C}$	M	-0.19	-0.06
12	$\frac{V}{V}$	M	0.18	0.12
13	$+\frac{}{T}$	M	-0.02	0.1
14	L	M	-0.02	0.08
15	Y	Н	0.44	
16	Q	Н	0.34	
$\frac{10}{17}$	S	Н	0.18	
18	W	Н	0.55	
19	R	Н	0.27	
20	Y	Н	0.44	
21	S	Н	0.18	
22	Q	Н	0.34	
23	A	Н	-0.0	
24	D	Н	-0.1	
25	N	M	0.1	
26	G	L	0.5	
27	C	L	-0.1	
28	A	L	0.0	
29	E	L	-0.1	
30	T	L	0.3	
31	V	M	0.1	
32	T	M	-0.0	
33	V	Н	0.0	2.00
34	K	Н	-0.2	
35	V	Н		
36	V	Н		
37	Y	Н		
38	E	M		
39	D	M	0.	28 4.30

40	D	M	0.28	4.64
41	T	M	-0.02	4.62
42	Е	M	0.14	4.76
43	G	M	-0.04	4.72
44	L	M	-0.02	4.7
45	С	M	-0.19	4.51
46	Y	Н	0.44	4.95
47	A	M	-0.04	4.91
48	V	M	0.18	5.09
49	A	M	-0.04	5.05
50	P	M	-0.1	4.95
51	G	L	0.53	5.48
52	Q	M	-0.04	5.44
53	I	L	-0.34	5.1
54	T	L	0.31	5.41
55	T	M	-0.02	5.39
56	V	M	0.18	5.57
57	G	M	-0.04	5.53
58	D	M	0.28	5.81
59	G	M	-0.04	5.77
60	Y	M	-0.09	5.68
61	Ī	L	-0.34	5.34
62	G	L	0.53	5.87
63	S	L	-0.06	5.81
64	H	L	0.3	6.11
65	G	L	0.53	6.64
66	Н	M	-0.43	6.21
67	A	Н	-0.02	6.19
68	R	Н	0.27	6.46
69	Y	Н	0.44	6.9
70	L	Н	0.18	7.08
71	A	Н	-0.02	7.06
72	R	Н	0.27	7.33
73	C	Н	0.24	7.57
74	L	Н	0.18	7.75

\* One of skill in the art recognizes that the Residue types are listed by the one letter amino acid designation.

<sup>a</sup> H, M, and L denote high, medium, and low stability as defined in the text and in footnote b of Table 3.

Value of the 3D-1D scoring matrix corresponding to the results of optimal alignment of the 2ait amino acid sequence given in the "Residue Type" column to the 1igd stability profile given in the "Stability Environment" column. These values are highly similar, but not identical, to the average values given in Table 3A because these values are from the scoring matrix produced when the target protein was removed from the database, as described in the text.

<sup>c</sup> Sum of all the values in the "3D-1D Matrix Score" column up to and including the indicated residue number. Values in boldface were used by the local alignment algorithm (Smith & Waterman, 1981) to compute the optimal sequence to profile alignment.

<sup>d</sup> Data in the "Cumulative Local Alignment Score" column was used to generate Figure 5C.

### Example 10 State of Ensemble Using COREX

[0104] A database of 81 proteins, 5849 residues total (Table 5), was selected from the Protein Data Bank (Baldwin and Rose, 1999) on the basis of biological and computational criteria as described previously in Example 1.

[0105] Next, the COREX algorithm (Hilser & Freire, 1996) was run with a window size of five residues on each protein in the database. The minimum window size was set to four, and the simulated temperature was 25 °C. The COREX algorithm generated an ensemble of partially unfolded microstates using the high-resolution structure of each protein as a template (Hilser & Freire, 1996) similar to Example 2. This was facilitated by combinatorially unfolding a predefined set of folding units (*i.e.*, residues 1 - 5 are in the first folding unit, residues 6-10 are in the second folding unit, etc.). By means of an incremental shift in the boundaries of the folding units, an exhaustive enumeration of the partially unfolded species was achieved for a given folding unit size (Hilser & Frieir, 1996; Wrabl, *et al.*, 2001).

[0106] Next, the Gibbs free energy for each state,  $\Delta G_i$  relative to the fully-folded reference state was calculated from surface area- and conformational entropy-based parameterizations described previously in Example 2 (Wrabl *et al.*, 2001). Thus, the  $\Delta G_i$ , of each state arises from differences in solvation of apolar and polar surface area, and from differences in conformational entropy between each state and the reference state. Therefore, dividing the free energy into its component terms gives:

$$\Delta G_i = \Delta G_{apolar,i} + \Delta G_{polar,i} + \Delta G_{confS,i} \tag{9}$$

[0107] As Equation 9 indicates, different values for the component contributions can provide similar magnitudes for  $\Delta G_i$ , suggesting that different states can have similar stabilities, but different mechanisms for achieving that stability.

Table 5. Proteins Used in the COREX Thermodynamic Database

<b>X-RAY</b> 17 2.3 62 62 62 67 NIMB
517 62 62
62 6
9 (9
6
70
5.2207 1 1.45
2.9454 53 NMR
2.5896 53
5.58 0.6515 617
0.7564 826
2.5997 98 1.85
3.5155 7 NMR
10.2 4.2561 18 NMR
6.6063 1 1.8
3.78 7 1.6
0.6685 872

		T		- T	T .		T	1	Τ		Γ	<u> </u>	Т		1			Τ-	
	SCOP files	Non-homologous(44)	Low Sequence	Non-	Non-	homologous(44) PDB Select	PDB Select		Non-	homologous (44)	PDB Select	SCOP files	SCOP files	I	Misc	PDR Soloct	ו הם סכוננו	SCOP files	PDB Select
	1	3	1	4	3	3	2		3		3	-	2		4	-	4	-	2
		1.9		NMR	1.7	1.5	2		2.6		1.5					~	?		2
	2	3508	-		2014	379	2	4	က		346	31	20		1255	-	•	7	2
	10.02 4.0935	4.42 -0.8659 3508	4.8891	3.98 -0.4757 2617	5.05 -0.0593 2014	6.68 1.5073	5.0183	9.68 3.8185	14.45 7.5708		1.5595	3.7289	8.64 2.3904		0.3324 1255	10.28 5.0104		10.72 4.9646	10.8 4.9686
	10.02	4.42	10.69	3.98	5.05	6.68	11.2	9.68	14.45		6.57	8.89	8.64		5.67	10.28		10.72	10.8
expression A	Annexin	P-loop containing NTP hydrolases	Cytochrome C	RING finger domain C3HC4	Alpha + beta Ribosomal protein L7/12 C-	Alpha+beta Cytochrome b5	Sm motif of small nuclear ribonucleonrofeins. SNRNP	SAM domain like	KH domain		SRF-like	N cbl like	N-terminal domains of the	minor coat protein g3p	Glutacorticoid receptor like	DNA/RNA-hinding 3-helical	bundle	Long alpha hairpin	alpha-Amylase inhibitor
	All Alpha	Alpha / beta	All Alpha	Small	Alpha+beta	Alpha+beta	All beta	All Alpha	Alpha+beta		+	All Alpha				proteins All alpha		All alpha	All beta
	73	77	83	89	89	88	81	69	73		71	77	22		72	52		77	74
	16 1BO9:A	17 1C1Y:B	1CC5:_	1CHC:_	1CTF:_	1CYO:_	1D3B:B	23 1DOQ:A	1DT4:A		25   1EGW:A	1E00:A	27 1FGP:_		1GDC:_	1HCR:A		1HDJ:	31 1HOE:_
	16	17	18	19	70	21	22	23	24		25	76	22		28	29		30	31

		_							····		-												$\neg$
SCOP_files	SCOP_files		Non	homologous(44)	Non-	homologous(44)	SCOP_files	Misc	PDB Select	SCOP_files	Misc	Non-	homologous (44)	Non-	homologous(44)	PDB Select	Misc	Non-	homologous(44)	Non-	homologous(44)	SCOP_files	SCOP_files
1	$\vdash$		4		4		1	3	3	2	-	7		4		4	3	1		1		2	-
			1.1		1.5			NMR	1.8			2		NMR		1.7		NMR		NMR			
13	19		28		_		_	168	443	63	13	24		20		2558	2302	1133		∞		3	355
4.1189	3.4092		2.422		5.3834		18.12 11.213	2.0885	1.099	2.8257	5.5138	2.8477		3.3845		3.47 -0.4586 2558	0.0759 2302	0.6857 1133		10.73 4.7036		6.2583	7.26 1.5261
11.43	8.8		7.57		10.71		18.12	7.29	6.26	9.22	12.97	8.31		8.58		3.47	5.25	9		10.73		13.77	7.26
p8-MTCPI	MHC class II extoplasmic	trimerization domain	Rubredoxin like		HipiP		Kix domain of CBP	Anaphylotoxins (complement system)	Alpha+beta Yeast killer toxins	PDZ domain like	EF Hand-like	OB fold		Midkine		MoMLV p15 fragment (residues 409-426)	SRCR-like	HMG box		Saposin		Crystallins proteins yeast killer	Alpha 2 macroglobulin receptor
All alpha	All Alpha		Small	proteins		proteins	۔ ا	All alpha	Alpha+beta	All Beta	All Alpha	All beta		Small	proteins	Peptides	Alpha+Beta SRCR-like	All alpha	ı	All alpha		All Beta	All alpha
89	22		53		62		81	74	63	88	88	69		59		53	96	62		78		88	81
32 1HP8:_	1IIE:A		34 11RO:_		1ISU:A		36 1KDX:A	1KJS:_	38 1KVE:A	39 1KWA:A	40 1MHO:_	41 1MJC:		42 1MKN:A		1MOF:_	44 1MWP:A	45 1NHM:_		46 1NKL:_		1NPS:A	48 1NRE:_
32	33		34		35		36	37	38	39	9	41		42		43	44	45		46		47	48

	786 1 SCOP_files	31 1.38 4 PDB Select		53 1.5 3 PDB Select		20 1.9 3. PDB Select	954 1.74 3 PDB Select	13 3 Misc	3 2 Low Sequence Identity	328 1.6 3 Non-	homologous(44)	348 1.95 4 PDB Select		9 1.3 4 Non-	homologous (44)	86 NMR 4 Non-	homologous (44)	252 1.63 3 PDB Select	114 NMR 1 Non-	mou	35 NMR 1 Non-	homologous(44)	100
	7.04 1.2342 7	3.7616		9.8 2.934		8.52 3.5069	6.05 0.4689 9	3.9136	8.607	6.95 1.4832 3		6.11 1.4565 3		11.22 4.9044		3.66 -0.1927 1886		6.42 1.6833 2	7.49 2.2425 1		5.47 0.3507 1035		0,,,,
associate protein (RAP) domain	FIS - like 7.0	Snake toxin-like 9.61			phosphocarrier proteins (HPr)		Alpha+beta Transcriptional coactivator 6.0	Alpha+Beta beta-Grasp (ubiquitin-like) 10.12	Cupredoxins 15.99	ta HPr proteins 6.		cys2, phorbol-	binding domain)	Knottins 11.		HIV-1 Nef protein fragments 3.		Alpha+beta Non-globular alpha beta 6.	E E	chicken villin	SIS / NS1 RNA binding domain 5.		011
	All Alpha	Small	Proteins	Alpha+beta		Alpha+beta	Alpha+beta	Alpha+Beta	All Beta	Alpha+beta	ı	Small	Proteins	Small	proteins	Peptides		Alpha+beta	All alpha	4	All alpha		
	91	62		85		59	99	56	66	87		50		64		99		<i>L</i> 9	29	•	56		
	1NTC:A	1NXB:_		10PD:_		10TF:A		1PGB:_	1PLC:_	56 1PTF:_		1PTQ:_		1PTX:_		1QA4:A		1QGW:B	100V:A		1R1B:A		
	49	50		51		52	53	54	55	56		57		58		59		09	61	•	62		

				T		7		7					<u> </u>				<del>(</del> +				4					
Misc	Misc	SCOP files	PDB Select		SCOP_files		Low Sequence	Identity	SCOP_files	PDB Select	PDB Select	Non	homologous (44)		PDB Select	Non	homologous (44)	PDB Select		Non	homologous (44)	PDB Select		SCOP_files		
	2		4		<b>—</b>		4			c	,  -	1	<u>^</u>		3	, \r	)	4	•	2		3		7		
			1.4							7.5	1.20	15.1	0.1		17	)	1	12		1.75		1.8				
-	9	-	503		243		73		317	46	2 +	- 0	7	33		41	-	67	)	က	•	9		-		
7.4941	6 0485	7 0584			1.5715		2.9194		1.6302	C 7740	0.77.0	1000	5.0864	0 40 2 4274	0.101.0	7.445	0.12 2.4332	0 4078	0.10	4 341	)	4.8841		6.45		
14.93 7.	1201 6				6.39		8.3		7.23 1		13.40		11.17	07 0	04.6	15.50	0.17	20 54 0 4078	40.0 <del>1</del>	11 24	7-7-1	10.98	)	13.15		15
nibitor/lipid-				Stalk segment of viral fusion	proteins	I AF II 230 II I DI DILIMINE	tragment	Ovomucold/FCr-1 like	Thermolvsin like metallo	proteases C-terminal domain		Ureroglobin-like	Alpha+beta DNA topoisomerase I domain		acyl CoA binding protein like	Alpha+beta Ferredoxin-like	Alpha+beta CI2 family of serine protease	inhibitors	BPTI-like		Beta clip	17	FKBP-like		Immunogiobuim-iike veta	Salidwincii
All Alpha		All beta			- 1	All alpha		Small	proteins All alpha	All alpha	Alpha+beta	All alpha	Alpha+beta	·	All Alpha	Alpha+beta	Alpha+beta		Small	Proteins	All beta		Alpha +	beta	All Beta	
91		57	74	62		29		99	S	70	82	0,0	2/22		98	85	65		58		99		84		6	
64  1RZL:		1SHG:	66 1SKN:P	1SVF:B		1TBA:A		1TGS:I	<.	Y	111GI:D	41 ITC:	73 1VCC:	1	74 2ABD:	75 2BOP.A	76 2CI2:1		77 2KNT:_		2SPG:A		79 3EIP:A		80 3NCM:A	
49	 - >	65	99	29		89		69		2	7	1 6	7 2	2	74	75	2/2	<u>-</u>	77	: 	78	<u>-</u>	79		8	

_		٦
DDR Select	ו חם סכונכנ	
_	<del>-</del>	
1 66	1.00	
7	_	
7 0040	15.08 7.9213	
20	15.08	
	Kringle-like	
	Small	Proteins
	84	
	81 5HPG:A	

### Example 11 Surface Area Calculations

[0108] The calorimetric enthalpy and entropy of solvation were parameterized from polar and apolar surface exposure (Hilser & Freire, 1996). COREX uses empirical parameterizations to calculate the relative apolar and polar free energies of each microstate:

$$\Delta G_{apolar,i}(T) = -8.44 * \Delta A S A_{apolar,i} + 0.45 * \Delta A S A_{apolar,i} * (T - 333) - T * (0.45 * \Delta A S A_{apolar,i} * ln(T/385))$$
(10)

$$\Delta G_{polar,i}(T) = 31.4.44 * \Delta ASA_{polar,i} - 0.26 * \Delta ASA_{polar,i} * (T - 333) - T * (-0.26 * \Delta ASA_{polar,i} * ln(T/335))$$
(11)

[0109] The three primary components used to calculate conformational entropies ( $\Delta S_{i,conf}$ ) for each microstate were: (1)  $\Delta S_{bu\to ex}$ , the entropy change associated with the transfer of a side-chain that was buried in the interior of the protein to its surface; (2)  $\Delta S_{ex\to u}$ , the entropy change gained by a surface-exposed side-chain when the peptide backbone unfolds; and (3)  $\Delta S_{bb}$ , the entropy change gained by the backbone itself upon unfolding (Hilser & Freire, 1996). For fold recognition calculations, the total ( $\Delta S_{i,conf}$ ) of all proteins is multiplied by a scaling factor to eliminate the unfolded state contribution to the residue-specific thermodynamic parameters.

[0110] Next, the residue stability constant,  $\kappa_j$ , was calculated similar to Example 2. The residue stability constant is the ratio of the summed probability of all states in the ensemble in which a particular residue, j, is in a folded conformation ( $\Sigma P_{f,j}$ ) to the summed probability of all states in which residue j is in an unfolded (*i.e.*, non-folded) conformation ( $\Sigma P_{nf,j}$ ).

[0111] Equation 2, in turn, was used to define a residue-specific free energy of folding for the protein  $(\Delta G_{f,j} = -RT \ln \kappa_{f,j})$ , which was expanded to give  $(\Delta G_{f,j} = RT \ln Q_{nf,j} - RT \ln Q_{f,j})$  where  $Q_{nf,j}$  and  $Q_{f,j}$  were the sub-partition functions for states in which residue j was unfolded and folded, respectively. Thus, the residue-specific free energy provides the difference in energy between the sub-ensembles in which each residue is folded and unfolded. In other words, the residue stability constant does not provide  $(\Delta G_{f,j} = RT \ln Q_{nf,j} - RT \ln Q_{f,j})$ 

the contribution of each amino acid to the stability of a protein. Rather, it provides the relative stability of that region of the protein, implicitly considering the contribution of all amino acids in the protein toward the observed stability at that position.

[0112] As shown in Figure 8, the stability constants provided a residue-specific description of the regional differences in stability within a protein structure. The importance of this quantity from the point of view of fold recognition is two-fold. First, the stability constant is compared directly to protection factors obtained from native state hydrogen exchange experiments, thus providing an experimentally verifiable residue-specific description of the ensemble. Second, as amino acids are non-randomly distributed across high, medium and low stability environments, the stability constant as a function of residue position provides a convenient 1-dimensional representation of the 3-dimensional structure.

## Example 12 Identification of Additional Thermodynamic Determinats

[0113] First, the  $\Delta G_i$  for each microstate i in the ensemble was composed of solvation and conformational entropy terms as described by Equation 9 and Example 10. Equation 9 was rewritten in terms of the enthalpic and entropic components:

$$\Delta G_{i} = \Delta H_{i, \text{ solvation}} - T(\Delta S_{i, \text{ solvation}} + \Delta S_{i, \text{ conformational}})$$
 (12)

[0114] Each of the solvation terms in Equation 12 was further expanded into contributions based on apolar and polar surface area:

$$\Delta G_{i} = (\Delta H_{i, \text{ solvation, apolar}} + \Delta H_{i, \text{ solvation, polar}}) - T(\Delta S_{i, \text{ solvation, apolar}} + \Delta S_{i, \text{ solvation, polar}}) - T(\Delta S_{i, \text{ conformational}}) (13)$$

[0115] However, the identical values for the apolar and polar areas of each state were used for the respective terms in the enthalpy and entropy calculations. Therefore, the absolute values for the enthalpy and entropy terms for a given area type were related by constants  $k_1$  (for apolar area) and  $k_2$  (for polar area), yielding the expression:

$$\Delta G_{i} = (\Delta H_{i, \, solvation, apolar} + \Delta H_{i, \, solvation, polar}) - T(k_{1}\Delta H_{i, \, solvation, apolar} + k_{2}\Delta H_{i, \, solvation, polar}) - T(\Delta S_{i, \, conformational})$$

[0116] Grouping area types together and simplifying gives:

$$\Delta G_{i} = [(\Delta H_{i, solvation, apolar}) * (1 - T * k_{1})] + [(\Delta H_{i, solvation, polar}) * (1 - T * k_{2})] - T(\Delta S_{i, conformational})$$
(15)

[0117] Equation 15 revealed that for a given free energy and conformational entropy, the relative contribution of polar and apolar surface to the solvation free energy was ascertained from the ratio of polar to apolar enthalpy for each state.

[0118] Thus, to arrive at a residue-specific contribution of polar and apolar solvation, a given thermodynamic parameter (i.e. enthalpy or entropy) is considered an average excess quantity, which represents the population-weighted contribution of all states in the ensemble. For instance, the average excess enthalpy and entropy was defined as:

$$\langle \Delta H \rangle = \sum_{i=1}^{N_{states}} P_i \bullet \Delta H_i = \sum_{i=1}^{N_{states}} \frac{K_i \bullet \Delta H_i}{Q}. \tag{16A}$$

$$\langle \Delta S \rangle = \sum_{i=1}^{N_{states}} P_i \bullet \Delta S_i = \sum_{i=1}^{N_{states}} \frac{K_i \bullet \Delta S_i}{Q}$$
 (16B)

[0119] Following from Equations 16A and 16B, residue-specific descriptors of the polar and apolar enthalpy were defined accordingly. The polar component of the enthalpy was defined as the difference between the average excess polar enthalpy from the sub-ensemble in which residue j is folded  $(\langle \Delta H_{pol,f,j} \rangle)$  and the average excess polar enthalpy from the sub-ensemble in which residue j is unfolded  $(\langle \Delta H_{pol,nf,j} \rangle)$ :

$$\Delta H_{pol,j} = \langle \Delta H_{pol,f,j} \rangle - \langle \Delta H_{pol,nf,j} \rangle$$
 (17)

where

$$<\Delta H_{pol,f,j}> = \sum_{i=1}^{N} \sum_{j=1}^{j, folded} \left( \frac{\left(\Delta H_{pol,f,i} \cdot e^{-\Delta G_i/RT}\right)}{Q_{f,j}} \right)$$
(18)

$$<\Delta H_{pol,nf,j}> = \sum_{i=1}^{N \ j,not \ folded} \left(\frac{\left(\Delta H_{pol,nf,i} \cdot e^{-\Delta G_i/RT}\right)}{Q_{nf,j}}\right)$$
 (19)

[0120] It is important to note that the summations in Equations 18 and 19 were only over the sub-ensembles in which residue j was folded and unfolded, respectively, and the parameters  $Q_{fj}$  and  $Q_{nfj}$  were the sub-partition functions for those sub-ensembles. By identical reasoning, the residue-specific apolar component to the enthalpy of residue j and the residue-specific conformational entropy component of residue j were defined as:

$$\Delta H_{apol,j} = \langle \Delta H_{apol,f,j} \rangle - \langle \Delta H_{apol,nf,j} \rangle \tag{20}$$

$$\Delta S_{conf,j} = \langle \Delta S_{conf,f,j} \rangle - \langle \Delta S_{conf,nf,j} \rangle$$
 (21)

As in the case with the residue stability constant, the expressions for the residue-specific  $\Delta H_{apol,j}$ ,  $\Delta H_{pol,j}$  and  $\Delta S_{conf,j}$  do not provide the contributions of residue j to the respective overall thermodynamic properties. Instead, Equations 17, 20 and 21 reflect the average thermodynamic environments of that residue, accounting implicitly for the contribution of all the amino acids over all the states in the ensemble.

#### Example 13 Residue-Specific Thermodynamic Environments

[0122] Using Equations 2, 17, 20, and 21, thermodynamic environments were empirically defined so as to systematically account for the different contributions of solvation and conformational entropy to the overall stability constant of each residue. As shown in Figure 9A-Figure 9C, three thermodynamic dimensions were considered; stability ( $\kappa_{f,i}$ ), enthalpy ( $H_{ratio,j}$ ), and entropy ( $S_{ratio,j}$ ). The first dimension utilizes the stability constant classification (Figure 8A and Figure 8B) defined by Equation 2. As the particular value for the stability constant can arise from conformational entropy or solvent related phenomena, a second dimension was utilized that provided the ratio of the conformational entropy to the total solvation free energy;

$$S_{ratio,j} = \frac{\Delta S_{conf,j}}{\Delta G_{solv,j}} \tag{22}$$

where  $\Delta G_{solv,i}$  is the total residue-specific solvation component [0123]calculated similar to Equations 17-21. Finally, as the total solvation component can arise 25112195.1

from polar or apolar contributions, a third dimension was incorporated that provided the ratio of polar to apolar enthalpy described by Equations 17 and 20;

$$H_{ratio,j} = \frac{\Delta H_{pol,j}}{\Delta H_{apol,j}} \tag{23}$$

[0124] Thus, the residues making up the 81 proteins (Table 5) that were analyzed partitioned non-randomly within the three-dimensional thermodynamic space. The non-random distribution of residues resulted in an empirical partitioning of the residue-specific data into twelve thermodynamic categories by dividing the stability data into three categories, the enthalpy data into two categories, and the entropy data into two categories (Figure 9A-Figure 9C).

## Example 14 Binning of Thermodynamic Environments

[0125] Each of the 5849 residues in the database were binned into one of the twelve thermodynamic environment classes based on their stability  $(\kappa_{f,j})$ , enthalpy  $(H_{ratio,j})$ , and entropy  $(S_{ratio,j})$  values. These thermodynamic environments were denoted by the following abbreviations: LLL, LLH, LHL, LHH, MLL, MLH, MHL, MHH, HLL, HLH, HHL, HHH. For example, residues in the LMH thermodynamic environment were binned into the Low (L) stability  $(\kappa_{f,j})$  class, the Medium (M) enthalpy  $(H_{ratio,j})$  class, and the High (H) entropy  $(S_{ratio,j})$  class. The cutoffs for each thermodynamic class were defined as:

Stability  $(\kappa_{f,j})$  class (L, M, or H):

-Low 
$$\kappa_{f,j}$$
 (L) = [  $\ln \kappa_{f,j} < 7.95$  ] (22)

-Medium 
$$\kappa_{fj}$$
 (M) = [ 7.95 <= ln $\kappa_{fj}$  < 13.4 ] (23)

-High 
$$\kappa_{f,j}$$
 (H)  $\equiv [13.4 <= \ln \kappa_{f,j}]$  (24)

Enthalpy  $(H_{ratio,i})$  class (L or H):

25112195.1

Low 
$$H_{ratio,j}$$
 (L) = [  $-\Delta H_{pol} < -1.024 * \Delta H_{ap} - 2553$  ] (25)

High 
$$H_{ratio,j}$$
 (H)  $\equiv$  [  $-\Delta H_{pol} > = -1.024 * \Delta H_{ap} - 2553$  ] (26)

Entropy  $(S_{ratio,j})$  class (L or H):

Low 
$$S_{ratio,i}$$
 (L)  $\equiv$  [  $-T\Delta S_{conf} < 0.125 * \Delta G_{solv} - 3053$  ] (27)

High 
$$S_{ratio,i}$$
 (H)  $\equiv$  [  $-T\Delta S_{conf} >= 0.125 * \Delta G_{solv} -3053$  ] (28)

[0126] Visual inspection of the segregation of amino acid types as a function of various thermodynamic parameters extracted from the 81-protein COREX database, guided by the development outlined above, suggested that the general classifications of stability, enthalpy, and entropy was reasonably divided thermodynamic space (as indicated in Figure 9). The exact cutoffs for the twelve residue-specific thermodynamic environments used in the threading calculations were determined automatically by an exhaustive grid search of all possible. The utility of each trial set of cutoffs was initially determined from a coarse search of cutoff space by threading a constant subset of 8 targets in the protein database and recording sets of cutoffs that maximized the Z-scores and percentiles for each target. Then, a finer grid search over the best sets of cutoffs, threading against a subset of 20 targets for each trial set of cutoffs, resulted in the optimized set of cutoffs used for the threading experiments shown in this work. Identical cutoffs were used for the alpha/beta threading calculations, *i.e.* no special optimization was performed for the scoring of the alpha/beta experiment.

[0127] Statistics for amino acid type as a function of each of the thermodynamic environments were tabulated (Table 6) and the log-odds probability for an amino acid type to be in each thermodynamic environment was calculated. The resulting histograms (Figure 10) revealed a non-random distribution of the amino acids within the thermodynamic environments. For example, hydrophobic residues such as Ile, Phe, and Val were observed with lower frequency in the MLL environment, while polar and charged amino acids such as Asp, Gln, and Lys were observed with higher frequency in this environment. These distributions cannot always be rationalized on the basis of side chain chemical properties, however, as the basic amino acids Arg and Lys exhibited very different propensities to occur in the MHL environment. This latter observation must be a reflection of the fact that ensemble-derived energetics included averaged tertiary enthalpic and entropic information that is not encoded by individual side chain properties alone.

25112195.1

Table 6. Statistics of Amino Acid Type as a Function of the Twelve Thermodynamic

environments	nents												
	LHH	LHL	нтт	1	MHH	MHL	MLH	MLL	HHH	HHL	НСН	HLL	SUM
ALA	48	19	26	30	74	24	55	44	53	15	99	22	466
ARG	12	10	14	13	29	4	23	37	28	13	28	40	281
ASN	=	တ	∞	20	20	13	40	46	12	10	22	41	252
ASP	14	16	16	32	30	24	41	75	21	10	25	27	331
CYS	2	5	5	20	12	4	14	37	11		18	36	174
GLN	4	5	7	13	12	13	28	34	21	19	38	42	236
GLU	17	30	16	42	38	47	34	20	30	25	44	53	446
GLY	32	55	21	11	39	41	38	79	12	6	15	16	434
HIS	9	8	4	12	11	2	12	14	17	9	13	9	114
	27	12	3	15	20	34	15	14	99	30	16	12	304
E	28	25	12	12	92	55	30	33	91	33	41	59	481
LYS	36	31	24	35	55	51	46	9/	38	29	42	45	208
MET	1-	4	8	7	16	15	10	19	14	13	ဝ	14	131
PHE	∞	10		9	30	25	က	က	48	29	10	10	182
PRO	45	18	77	17	9/	17	22	13	7	1	7	က	241
SER	19	13	13	26	41	13	53	42	31	6	44	29	333
THR	23	22	13	32	44	36	37	41	21	15	14	14	312

4 / 1	23 163	-	7000	_	t	482 2849	ᅥ		
9	11 2		_	ري -	+	524 4	_		
71	CC	ر ا	,	73		227			
13	3	 40 		7	•	000	000		
က		_		った	2	100	)     		
		C.	,	76	†		553		
7		20	2	00	က က		47q	) 	
7	•	17	_	3	84		707		
C	0	7	_		- - -	3	367	430	
			_		<del>ر</del>	7		214	
	2		ی	>	7	7		315	
	~	-	7	 -	3	45		385	
	100		0>+					2	

### **Example 15 Fold-Recognition Details**

[0128] Simple fold-recognition experiments were performed based on amino acid distributions within the twelve thermodynamic environments.

[0129] Briefly, a profiling method was used to create thermodynamic environment profiles for each of the 81 proteins in the database (Bowie et al., 1991; Gribskov et al., 1987). The 81 amino acid sequences (Table 5) coding for the native structures used in the database (in addition to 3777 decoy sequences) were each threaded against the 81 target thermodynamic environment profiles. The decoy sequences were obtained from the Protein Data Bank and were inclusive for all sequences coding for "foldable" proteins ranging from 35 to 100 residues.

[0130] Next, a 3D-1D scoring matrix for each protein in the database was calculated, in which the scoring matrix data was simply the log-odds probabilities of finding amino acid types in one of the thermodynamic environment classes (Equation 30, below). The resulting profile of the target protein was then optimally aligned to each member of a library of amino acid sequences (i.e. 3858 decoy sequences) by maximizing the score between the sequence and the profile using a local alignment algorithm based on the Smith-Waterman algorithm (Smith & Waterman, 1981) as implemented in PROFILESEARCH (Bowie et al., 1991). No attempt was made to optimize the gap opening and extension penalties for the local algorithm; in all cases these were the default values given in the PROFILESEARCH package, 5.00 and 0.05, respectively. Z-scores were computed from PROFILESEARCH for each threading result from Equation (30):

$$Z = (s-\sigma)/\langle S \rangle \tag{30}$$

[0131] In Equation 30, s was the PROFILESEARCH threading score of a sequence i when threaded against the structure corresponding to sequence i, <S> was the average threading score of all sequences in the database (identical in length to sequence i) threaded against the structure corresponding to sequence i, and  $\sigma$  was the standard deviation of the scores of all sequences in the database (identical in length to sequence i) threaded

against the structure corresponding to sequence i. Thus, the Z-score was the number of standard deviations above the mean that sequence i scored against its target.

[0132] Nearly three-fourths (60/81) of the correct sequences scored in the top 5<sup>th</sup> percentile when threaded against their corresponding thermodynamic environment profile (Figure 10), and the Z-scores (the number of standard deviations a particular sequence scored above the mean score of all chains of identical length) for these successful threadings ranged from 1.76 to 12.23 (Table 7).

Table 7. Fold Recognition Results

Labi	e 7. Fold is		
No.	PDB	% Rank Z	
1	1A1I:A	0.29	3.49
2	1A6S:_	0.67	3.23
3	1A8O:_	0.34	3.29
4	1AA3:_	3.84	2.08
5	1ABA:_	0.03	4.1
6	1ADR:_	0.93	3.71
7	1AIW:_	2.36	2.27
	1AN4:A	23.64	0.68
9	1AOI:B	26.31	0.52
	1AVY:C	5.16	1.82
11	1B9G:A	0.18	4.48
	1BDD:_	0.44	5.07
13	3 1BDO:_	0.05	6.25
	11BF4:A	0.16	4.04
15	1BG8:A	33.23	0.32
16	6 1BO9:A	0.21	4.06
1	7 1C1Y:B	95.44	-1.46
18	3 1CC5:_	0.13	5.3
19	9 1CHC:_	67.88	-0.55
2	0 1CTF:_ 1 1CYO:_	32.17	0.22
2	1 1CYO:_	5.47	1.76
	2 1D3B:B	0.93	
	3 1DOQ:A	0.03	
	4 1DT4:A	0.08	
	5 1EGW:A		
	6 1EO0:A	0.88	
2	7 1FGP:_	2.13	
	8 1GDC:_	64.41	
	9 1HCR:A	0.16	
	31 1HOE:_	0.13	5.62
	30 1HDJ:_ 31 1HOE:_	1.35 0.13	

No.	PDB		Z_SCORE
41	1MJC:_	4.07	1.99
42	1MKN:A	3.24	2.33
	1MOF:_	65.34	-0.47
44	1MWP:A	24.29	0.56
45	1NHM:_	17.26	0.93
46	1NKL:_	0.91	3.19
47	1NPS:A	0.13	
	1NRE:_	24.29	0.54
49	1NTC:A	39.71	
50	1NXB:_	0.78	
	10PD:_	4.15	
52	10TF:A	1.09	
53	1PCF:A	40.95	
54	1PGB:_	0.13	
55	1PLC:_	0.13	
56	SIPTF:	7.34	1.63
57	7 1PTQ:_	9.62	
58	3 1PTX:_	0.47	
5	9 1QA4:A	45.59	-0.05
6	0 1QGW:E		
6	1 1QQV:A		
	2 1R1B:A	22.70	
6	3 1ROP:_	42.4	
-	4 1RZL:_	0.0	
	5 1SHG:_	0.0	
	6 1SKN:P		
	7 1SVF:B		
	8 1TBA:A		9 2.68
	9 1TGS:I	2.6	
1 .	'0 1TRL:A		4 0.53
7	1 1UGI:D	0.4	4 7.02

0.47	4.43
0.39	3.28
0.13	5.4
0.54	3.58
0.03	9.34
32.4	0.26
2.41	2.5
0.29	3.7
0.39	3.54
	0.39 0.13 0.54 0.03 32.4 2.41

72 1UTG:	0.08	5.92
73 1VCC:	0.08	4.48
74 2ABD:_	0.23	3.96
75 2BOP:A	0.03	7.09
76 2CI2:I	5.44	2.06
77 2KNT:_	0.08	12.23
78 2SPG:A	0.39	5.31
79 3EIP:A	0.18	5.53
80 3NCM:A	0.44	4.24
81 5HPG:A	0.05	11.02

## Example 16 Construction of Scoring Matrices

[0133] The scoring matrices were calculated as log-odds probabilities of finding residue type j in structural environment k, as described below (Wrabl  $et\ al.$ , 2001; Bowie  $et\ al.$ , 1991). The matrix score,  $S_{j,k}$ , was defined as:

$$S_{j,k} = \ln \frac{P_{j|k}}{P_k} \tag{27}$$

## Example 17 Thermodynamic Information is more Fundamental than Secondary Structure Information

[0135] Secondary structure, although useful in the analysis and classification of protein folds, is an easily reportable observable that does little to explain the underlying physical chemistry of protein structure. In fact, secondary structure can be viewed as a manifestation of the backbone/side-chain van der Waals' repulsions that divide phi/psi space, modified by the thermodynamic stability afforded by local and tertiary interactions such as hydrogen bonding and the hydrophobic effect (Srinivasan & Rose, 1999; Baldwin & Rose, 1999). Any reasonable description of the energetics of protein structure must be able to reflect these realities independent of secondary structural propensities of amino acids and the secondary structural classifications of folds.

- [0136] Although the COREX energy function accounts for specific interactions only in an implicit way, the results of a COREX calculation may provide deeper insight than secondary structure into the structural determinants of protein folds. For example, Figure 9C compared the thermodynamic environment profiles for an all-alpha protein and an all-beta protein threaded over their native folds. Visual inspection of the two color-coded structures revealed that different thermodynamic environments span single types of secondary structure, and that the same thermodynamic environment was found in different types of secondary structural elements.
- [0137] Thus, a threading procedure was repeated on a subset of proteins from the original database (Table 5), sorted by secondary structure to determine the possibility that the thermodynamic environments calculated by COREX represented a fundamental property of proteins that transcended structural classifications.
- [0138] First, a scoring table was assembled from the 31 proteins in Table 5 that were classified by the SCOP database as being "All alpha" proteins. Second, the 12 "All beta" proteins from Table 5 were threaded using the scoring table derived solely from the "All alpha" proteins. In other words, amino acid propensities for the thermodynamic environments from all-alpha proteins were used to perform fold recognition experiments on all-beta proteins. For more than 80% of the targets (10/12), sequences known to adopt the native all-beta structures scored in the top 5% of the 3858 decoy sequences, (Figure 12).

[0139] This result was a clear demonstration that the energetic information derived from the COREX calculations was independent of protein secondary structure.

25112195.1 · 59

#### REFERENCES

[0140] All patents and publications mentioned in the specification are indicative of the level of those skilled in the art to which the invention pertains. All patents and publications are herein incorporated by reference to the same extent as if each individual publication was specifically and individually indicated to be incorporated by reference.

Altschul et al., 1997, Nuc Acid Res 25: 3389-3402.

Anfinsen CB. 1973, Science 181: 223-230.

Bai & Englander, 1996, Proteins 24: 145-151.

Baker et al., 1992, Nature 356: 263-265.

Baldwin RL. 1986, Proc Natl Acad Sci USA 83: 8069-8072.

Bowie et al., 1991, Science 253: 164-170.

Chamberlain et al., 1996, Nat Struct Biol 3: 782-788.

Cohen FE. 1999, J Mol Biol 293: 313-320.

D'Aquino et al., 1996, Proteins 22: 404-412.

Feldman & Frydman J. 2000, Curr Opin Struct Biol 10: 26-33.

Fink AL. 1999, Physiol Rev 79: 425-449.

Gomez et al., 1995, Proteins 22: 404-412.

Gribskov et al., 1987, Proc Natl Acad Sci USA 84: 4355-4358.

Habermann & Murphy. 1996, Prot Sci 5: 1229-1239.

Hilser & Freire. 1996, J Mol Biol 262: 756-772.

Hilser et al., 1998, Proc Natl Acad Sci USA 95: 9903-9908.

Hobohm & Sander. 1994, Prot Sci 3: 522-524.

Huyghues-Despointes et al., 1999, Biochem 38: 16481-16490.

Jackson, 1998, Fold Des 3: R81-91.

Jaravine et al., 2000, Prot Sci 9: 290-301.

Jones et al., 1999. Proteins Suppl 3:104-111.

Kabsch & Sander. 1983. Biopolymers 22: 2577-2637.

Kuroda & Kim. 2000. J Mol Biol 298: 493-501.

Lee et al., 1994. Proteins 20: 68-84.

Llinas et al., 1999. Nat Struct Biol 6:1072-1078.

Murzin et al., 1995. J Mol Biol 247: 536-540.

25112195.1 60

Pan et al., 2000. Proc Natl Acad Sci USA 97: 12020-12025.

Park et al., 1998. J Mol Biol 284: 1201-1210.

Pereira et al., 1999, Biophys. J. 76:2319-2328.

Pochapsky & Gopen. 1992. Protein Sci. 1:786-795.

Rice & Eisenberg. 1997. J Mol Biol 267: 1026-1038.

Sadqi et al., 1999. Biochem 38: 8899-8906.

Smith & Waterman. 1981. J Mol Biol 147: 195-197.

Swint-Kruse & Robertson. 1996. Biochem 35: 171-180.

Xie & Freire. 1994. J Mol Biol 242: 62-80.

Wrabl, et al., Protein Sci 10(5) 1032-45.

[0141] Although the present invention and its advantages have been described in detail, it should be understood that various changes, substitutions and alterations can be made herein without departing from the spirit and scope of the invention as defined by the appended claims. Moreover, the scope of the present application is not intended to be limited to the particular embodiments of the process, machine, manufacture, composition of matter, means, methods and steps described in the specification. As one of ordinary skill in the art will readily appreciate from the disclosure of the present invention, processes, machines, manufacture, compositions of matter, means, methods, or steps, presently existing or later to be developed that perform substantially the same function or achieve substantially the same result as the corresponding embodiments described herein may be utilized according to the present invention. Accordingly, the appended claims are intended to include within their scope such processes, machines, manufacture, compositions of matter, means, methods, or steps.

61

25112195.1